Science of the Total Environment 817 (2022) 152807

Contents lists available at ScienceDirect

Science of the Total Environment

journal homepage: www.elsevier.com/locate/scitotenv

Impacts of dissolved Zn and nanoparticle forms in the fatty acid landscape of *Mytilus galloprovincialis*

Joana Roma [a,*], Eduardo Feijão [a], Catarina Vinagre [a,b], Bernardo Duarte [a,c], Ana Rita Matos [c,d]

[a] MARE - Marine and Environmental Sciences Centre, Faculdade de Ciências da Universidade de Lisboa, Campo Grande, 1749-016 Lisbon, Portugal.
[b] CCMAR, Centre of Marine Sciences, Universidade do Algarve, Campus de Gambelas, 8005-139 Faro, Portugal.
[c] Departamento de Biologia Vegetal, Faculdade de Ciências da Universidade de Lisboa, Campo Grande, 1749-016 Lisboa, Portugal.
[d] BioISI - Biosystems and Integrative Sciences Institute, Plant Functional Genomics Group, Departamento de Biologia Vegetal, Faculdade de Ciências da Universidade de Lisboa, Campo Grande, 1749-016 Lisboa, Portugal.

HIGHLIGHTS

- Both zinc forms are able to alter FA composition in *M. galloprovincialis*.
- Even small concentrations in longer exposures can have an impact.
- Possible consequences on the feasibility of contaminated mussels as a food source
- FA profile changes were used as a biomarker for zinc nanotoxicity in mussels.

GRAPHICAL ASBSTRACT

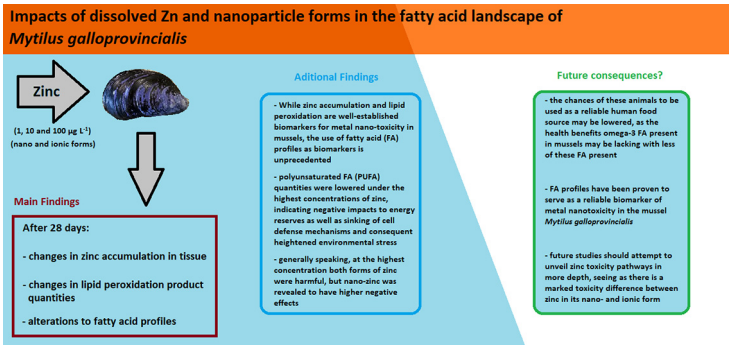

ARTICLE INFO

Article history:
Received 27 July 2021
Received in revised form 27 December 2021
Accepted 27 December 2021
Available online 10 January 2022

Editor: Daniel Wunderlin

Keywords:
Mytilus galloprovincialis
Zinc
Fatty acids
Lipid peroxidation
Nanotoxicity
Heavy metal toxicity

ABSTRACT

The introduction of waste containing heavy metals into the marine environment has been increasing for the past few decades, yet there are still several pending questions regarding how it impacts aquatic fauna. This study compared the effects of zinc exposure in its ionic- and nanoparticle forms on the mussel *Mytilus galloprovincialis* and sampled at different time-points. Zinc accumulation was observable after one week. Exposure to 100 µg L^{-1} of either form for 28 days also resulted in the higher depletion of fatty acids, lipid peroxidation products accumulation, and changes in the fatty acid profiles. This was also observed for lower concentrations, although to a smaller extent. Given the importance of fatty acids in the marine trophic chains, these zinc-induced alterations have significant potential of introducing negative impacts on the ecosystem and ultimately on human nutrition. Finally, we show that fatty acids may be used as efficient biomarkers of zinc-induced stress.

* Corresponding author.
E-mail address: jcroma@fc.ul.pt (J. Roma).

http://dx.doi.org/10.1016/j.scitotenv.2021.152807

1. Introduction

Waste containing metals is often discharged into the marine environment, imposing severe wellness hazard to living organisms (Nadella et al., 2009). Trace metal elements can cause varying degrees of toxicity in marine biota, highly dependent on their physical and chemical characteristics (Bhatt and Tripathi, 2011), and once inside an organism, metals can cause a plethora of damages, often due to the triggering of an excess of reactive oxygen species (ROS) through Fenton-type reactions, that will target lipids, proteins and DNA (Baker et al., 2014).

While already many biochemical and physiological issues are known to be induced in living organisms by the ionic form of metals, less information is available regarding their nanoparticulate form, although a similar or even higher potential for damage is predicted due to their small dimensions (1–100 nm per dimension) (Organisation for Economic Co-operation and Development - OECD, 2009; Franzitta et al., 2020). These particles are some of the most important anthropogenically produced nanomaterials nowadays due to their wide commercial use (Baker et al., 2014). As such, they also present rather unique risks due to their size as opposed to their larger ionic counterparts: their small surface to volume ratio and surface charge (which increase both their reactivity and mobility) are often deemed highly likely to induce harm within the natural environments they are introduced into, if in excess of this same environments' needs for this metal (Schrand et al., 2010).

However, due to the difficulties associated with the detection and quantification of very small yet highly reactive particles, there is still a considerable lack of data on the exact impact of metal nanoparticles and dissolved metal pollution: as such, nanotoxicity researchers have begun prioritizing alternative ways to characterize the presence and impact of these in the environment: so far one of the best candidates is the surveillance of signs of abiotic and biotic changes in the environment (Ofiara and Seneca, 2006; Fox et al., 2016; Avila et al., 2018), through the use of biomonitors. The vast majority of studies using this method in marine research focus on crustaceans and molluscs as biomonitors (e.g. Zamuda and Sunda, 1982; Chong and Wang, 2009; Nadella et al., 2009; Fabrega et al., 2012; Taze et al., 2016), but occasionally fish are used as well (e.g. Sunda et al., 1978; Vignardi et al., 2015; Li et al., 2018). By using biomonitors, researchers can look at biomarkers, which are measurable biological parameters at the subindividual (genetic, enzymatic, physiological, morphological) level where functional or structural changes occur, that can indicate general environmental influences (Markert et al., 2003).

Zinc was highlighted by the OECD as one of the metals introduced anthropogenically with the highest interest as a construction material due to its widespread use and commercial importance and inherent properties (OECD, 2009). Zinc presents strong adsorption ability and is noted for its chemical stability (Osmond and McCall, 2010). Zinc nanoparticles are found in paints, cosmetics, animal feeds and fertilizers, and they are commonly components of sunscreens, as they are able to block UV light thus protecting skin cells (OECD, 2009). Widespread and ever-expanding production and use of zinc has compelled some researchers to quantify it in aquatic media: Keller et al. (2013), who modelled world-wide releases of several metal nanoparticles, estimated that zinc alone would contribute 170–2985 tons/year to receiving water bodies of all kinds. In 2020 zinc NP concentrations in European surface waters were predicted to be around 1 mg L^{-1} by Coll et al. (2016), while Gottschalk et al. (2009) reported also for Europe nano-zinc concentrations of 10 ng/L in natural surface water and 430 ng/L in treated wastewater, and lastly Van Sprang et al. (2009) measured concentrations in river waters that went up to 71.4 ng/L. Previous studies have shown that zinc in moderate/low concentrations is beneficial for most living organisms, however in high concentrations it is toxic to microorganisms, plants, aquatic biota and rodents (Brayner et al., 2006; Lin and Xing, 2007; Premanathan et al., 2011; Reddy et al., 2007; Wang et al., 2008; Santos et al., 2014; Duarte et al., 2021b). Zinc nanoparticles have also been often used in studies related to nanotoxicology in marine fauna (e.g. Wong et al., 2010; Manzo et al., 2013; Wong and Leung, 2014).

To conduct the present study, a common biomonitor was used: the mussel *Mytilus galloprovincialis*. Sessile filter-feeders are often used as biomonitors due to their sessile nature and ability to accumulate toxins in their tissues (Rainbow and Phillips, 1993) and often they act as the most effective sinks for metals in the estuarine and marine food webs (Parks et al., 2013). The bivalve taxa have been used as common choice biomonitors for many years (Rainbow et al., 2002), and mussels in particular are capable of tolerating significant fluctuations in temperature, salinity and oxygen concentrations, which combined with their abundance and annual availability makes them excellent bioindicators (Goldberg, 1986). Several experimental and laboratory studies have demonstrated that mussels also accumulate trace metals proportionally to their environmental availability (e.g. Boening, 1999). Among the available tissues, the mantle was chosen as the target tissue for this experiment for two reasons: this tissue is the first point of contact with pollutants, and while it serves as a protective layer for most of other organs, if it is negatively affected then the rest of the body is equally compromised (Mansom and Grover, 2018); and lastly there are very few studies that focus specifically on this tissue (Roma et al., 2020), which is why more information is needed in order to understand the full scope of how pollutants affect the mussel *M. galloprovincialis*.

Furthermore, seafood, where mussels are included, represent not only an important trophic segment of the marine food webs (Nielsen and Maar, 2007), but also an important aspect of a healthy human diet, as a protein, vitamin and mineral source (Monroig and Kabeya, 2018). They are also rich in the so-called “omega-3” (n-3) long-chain (C20–24) polyunsaturated fatty acids (PUFAs), which have been shown to be beneficial to several conditions including cardiovascular disease, many inflammatory illnesses, and some types of cancer (Brouwer et al., 2006).

In order to understand the impact of metal pollution, specific biomarkers such as accumulation of the metal on animal tissue, as well as lipid peroxidation and changes in fatty acid profiles are often used. In our study we have chosen fatty acids as biomarkers as they are still understudied namely on marine biota, despite being considered highly relevant for human diet. This study can serve as a stepping-stone for similar studies regarding changes in fatty acids in marine biota and how these can be critical biomarkers in pollution studies. Recent studies by our team have used these same biomarkers in several studies with other species (Duarte et al., 2021a, 2021b).

Starting with accumulation of pollutants inside an organism, the vast majority of ecotoxicity studies look at this factor as a common endpoint of toxicity, as metals may easily bind to the surface of or enter cells through endocytosis, for particles up to 100 nm in size (Iversen et al., 2011).

It is also well established that pollutants are capable of inducing changes in lipid metabolism and fatty acid profiles (Berge and Barnathan, 2005; Dailianis, 2011), such as alterations in the proportion of saturated vs unsaturated fatty acids as well as LC-PUFA contents (Labarta et al., 2005; Rocchetta et al., 2014). Lipid peroxidation occurs due to the interaction of metal-generated ROS and PUFAs, resulting in oxidative damage to these molecules and production of malondialdehyde (MDA) as the most abundant lipid peroxidation product (Pryor and Stanley, 1975). Changes to phospholipids and triglyceride synthesis and mobilisation (Viarengo et al., 2007), as well as membrane fluidity (Hannam et al., 2010), are also seen as viable indicators of toxicity.

To date no study has been carried out comparing the effects of zinc on both nanoparticle and ionic forms on the mussel *M. galloprovinciallis*. This study does that, while also testing long-term exposure time with different endpoints. In fact, the majority of metal ecotoxicity studies found in the literature last less than 2 weeks and seldom investigate several exposure intervals outside that range, which does not inform about realistic longer-term exposure to, for instance, effluents containing these metals that invade natural habitats for weeks and sometimes months at a time, continuously. Thus, there are still quite a few gaps in literature relating to long-term continuous exposure and the evolution/progression of the nanotoxicity involved.

This study evaluated and compared the impact of different concentrations of zinc, both the dissolved metal and the nanoparticles form, on

lipid peroxidation and fatty acids contents and profiles, in the mussel *M. galloprovinciallis* during a 28-day period, as well as identified potential biomarkers of exposure to different forms and concentrations of zinc in a marine sentinel organism. The hypothesis here tested is that elevated concentrations of zinc in ionic and nanoparticulate forms can cause accumulation in tissue which will then in turn cause damage to lipids and fatty acids. In order to test this, we performed total X-ray fluorescence spectroscopy element analysis to observe the rates of metal accumulation, quantification of lipid peroxidation products through the thiobarbituric acid reacting substance protocol, and finally fatty acid profiling using gas chromatography.

2. Materials and methods

2.1. Experimental setup

Mytilus galloprovincialis mussels were provided by Testa & Cunhas, a certified seller, which farms this species in oceanic rafts, offshore, in pristine waters (37°04,200′N 8°42,800′W, 37°04,200′N 8°41,000′W, 37°03,400′N 8°41,000′W, 37°03,400′N 8°42,800′W) at Ponta da Piedade, Lagos, Algarve region in Portugal. Two hundred mussels (mean length of 5.6 ± 0.38 cm and a mean weight of 16.6 ± 0.3 g) were immediately transported to a wet lab at Faculdade de Ciências da Universidade de Lisboa (FCUL) and evenly distributed into 12 acclimation aquaria (12 L each) on a closed water circulation system for a week, both to acclimatise them and to ensure that no mussels in poor physical condition would be used for the experiment. The water temperature was between 21 and 21.5 °C (±0.5 °C), the photoperiod was 12 h light/12 h dark and salinity was maintained at 35 ppm.

After acclimation, mussels were distributed into individual experimentation aquaria (10 individuals in each 12 L aquaria). Temperature, salinity and photoperiod during experimentation were similar to the acclimatization period. Immersible air bubblers stones, connected to air pumps by clear tubes, ensured both proper oxygenation as well as homogenous mixing of the water inside the aquaria to avoid the formation of metal deposits. During the experiment mussels were fed with *Phaeodactylum tricornutum* Bohlin (Bacillariophyceae; strain IO 108–01, IPMA) cells, cultured in our laboratory (Feijão et al., 2020), ad libitum every 3 days. Ammonia levels were monitored daily to guarantee that the mussels remained in good physical condition.

In order to verify the effects of zinc, 9 treatments were performed, with 4 aquaria per treatment, as such: 4 aquaria had no metals added (control treatment), 4 aquaria had 1 μg L^{-1}, 4 had 10 μg L^{-1}, and 4 had 100 μg L^{-1} of zinc. This experimental setup was used with ionic zinc and with nano-zinc. At days 0, 7, 14, 21 and 28 of the experiment, 2 mussels were collected from each aquarium (for a total of 10 per treatment), dissected and their mantle edge tissue immediately frozen in liquid nitrogen and stored at −80 °C for later analyses. The mantle edge was chosen as the target tissue, instead of the entirety of the mantle, to avoid gonadal tissue, as both of these tissues are connected except at the very edge of the mantle.

Ionic zinc was supplied in the form of $ZnSO_4$ (Sigma-Aldrich, Catalogue number 1724769), while nano-zinc was supplied as ZnO nanoparticles with a particle size less than 50 nm and a surface area of 10.8 m^2g^{-1} (Sigma-Aldrich, Catalogue number 677450). Zinc was added to the aquariums in target concentrations, starting from $ZnSO_4$ and ZnO stock solutions (10 mg L^{-1} of zinc) using the proper volumes to attain the target desired concentrations. Zinc concentration in the stock solutions were confirmed by Total Reflection X-ray Fluorescence (TXRF) spectroscopy (data not shown). The low volumes transferred from the stock solution to the aquariums, to attain the desired Zn concentrations, compared to the total aquarium volume were found to be very reduced and without effects in the pH of the system.

2.2. Zinc nanoparticle characterization

ZnO nanoparticles, dissolved in distilled water in a final concentration of 40 mg L^{-1}, were sonicated for 30 min, prior to dropcasting on 40 nm gold sputtered silicon substrates. Samples were air dried and then mounted on microscope stubs and grounded with Electrodag silver paint and copper tape. A dual-beam focused ion beam scanning electron microscope (SEM; FEI, Oregon, USA) was used to record zinc nanoparticles. Particle zeta potential was determined in experimental concentrations of zinc dissolved in seawater at the Nanophotonics and Bioimaging Facility of the International Iberian Nanotechnology Laboratory (Braga, Portugal), using a Dynamic Light Scattering System (DLSS; model SZ-100Z, Horiba Seisakusho, Japan). Zinc particle size distribution was surveyed using DLSS and through SEM (Suppl. Fig. S1A–D). Particle elemental composition and X-ray fluorescence spectra was obtained from the ZnO nanoparticles in seawater using TXRF as abovementioned (S2 PICOFOX, Bruker, Germany) (Suppl. Fig. S1E).

2.3. Element analysis and quantification

About 100 mg of sample were lyophilized and submitted to an acid digestion in digestion reactors (Teflon bombs) in the presence of 0.2 mL $HClO_4$ and 0.8 mL HNO_3 at 110 °C for 3 h (Sghaier et al., 2016). Once cooled, 496 μL of the digested samples were recovered and 4 μL of Ga (final concentration 1 mg L^{-1}) added as the internal standard for heavy metal quantification (Towett et al., 2013), and stored at 4 °C until analysis.

Heavy metal quantification was achieved with the aid of Total Reflection X-ray Fluorescence (TXRF) spectroscopy element analysis. Cleaning and preparation of the TXRF quartz glass sample carriers were performed according to Towett et al. (2013), with 5 μL of the digested sample added to the centre of the carrier. The carriers with the samples were aligned in a support containing a carrier with arsenic for gain correction (mono-element standard, Bruker Nano GmbH), a carrier with a nickel standard for sensitivity and detection limit (mono-element standard, Bruker Nano GmbH), and a carrier with a multi-element kraft for quantification accuracy (Kraft 10, Bruker Nano GmbH). Element measurements were made in a portable benchtop TXRF instrument (S2 PICOFOX™ spectrometer, Bruker Nano GmbH) for 800 s per sample. The accuracy and precision of the analytical methodology for elemental determinations were assessed by replicate analysis of certified reference material BCR-146. Blanks and the concurrent analysis of the standard reference material were used to detect possible contamination/losses during analysis. The TXRF spectra and data evaluation interpretation were performed using the Spectra 7.8.2.0 software. The efficiency of the extraction and analytical procedure was ensured through the analysis of certified reference material (Mussel tissue ERM-CE278k provided from the Institute for Reference Materials and Measurements, Zn extraction and analysis efficiency between 97.7 and 109.4%).

2.4. Quantification of lipid peroxidation products

Quantification of lipid peroxidation products was performed through the thiobarbituric acid (TBA) reacting substance (TBARS) protocol (Hodges et al., 1999). One hundred mg of frozen mussel mantle edge was homogenized with quartz sand in 80% ethanol (v/v) and centrifuged at 4 °C for 5 min at 14,000 ×*g*. The supernatants were mixed with a TBA solution in the presence of butylhydroxytoluene and heated at 95 °C for 30 min. Once cooled, samples were centrifuged at 14000 ×*g* for 10 min, and the supernatant was collected and analysed in a spectrophotometer. Absorbance was recorded at 532 nm wavelength and used to calculate the concentration of TBARS, using a calibration curve prepared with 1,1,3,3-tetraethoxypropane and expressed in nmol of MDA equivalents per g of fresh mussel tissue.

2.5. Fatty acid profiles

Total lipids were extracted from 400 mg of mussels' mantle edge pooled from 4 individuals for the same experimental condition. Three replicates per treatment were performed. Samples were homogenized with quartz sand in a mortar and pestle and extracted with a methanol/chloroform/water (1:1:1) mixture (Feijão et al., 2020). Samples were vortexed and

centrifuged at room temperature for 10 min at 1800 ×*g*. The organic phase containing the lipids was recovered. The upper phase was re-extracted by adding chloroform and repeating the above-described process. Both lipidic fractions were combined and dried under a stream of nitrogen at 37 °C. Lipids were re-suspended in an ethanol-toluene solution (1:4) under nitrogen atmosphere at −20 °C until analysis. Fatty acid profiling was performed by trans-esterification of lipid samples in methanol-sulfuric acid (97.5%, v/v) at 70 °C for 60 min, as described in Feijão et al. (2018) and Duarte et al. (2019), with pentadecanoic acid (C15:0) used as an internal standard. Fatty acid methyl esters (FAMEs) were recovered with petroleum ether, dried under an N_2 flow and re-suspended in an appropriate amount of hexane. One microliter of the FAME solution from each sample was analysed in a gas chromatograph (430 Gas Chromatograph, Varian) equipped with a hydrogen flame ionization detector set at 300 °C. The temperature of the injector was set to 270 °C, with a split ratio of 50. The fused-silica capillary column (50 m × 0.25 mm; WCOT Fused Silica, CP-Sil 88 for FAME; Varian) was maintained at a constant nitrogen flow of 2.0 mL min^{-1}, and the oven temperature was set at 190 °C. FA identification was performed by comparing retention times with standards (Sigma-Aldrich), and chromatograms analysed by the peak surface method using the Clarity 7.4 software (DataApex), permitting us to obtain fatty acid profiles for the 28th day of the treatments nano-zinc and ionic zinc at 10 and 100 μg L^{-1} as well as control. Furthermore, specific relevant indexes resulting from the characterization of fatty acids were calculated, as these were the Double Bond Index (DBI), IT (Index of Thrombogenicity) and IA (Index of Atherogenicity), the formula for the first was taken from Fonseca et al. (2021) and the formulas for the last two Indexes were taken from the work of Ulbricht and Southgate (1991). These were calculated as follows:

$$\mathrm{DBI} = (2 \times ((\Sigma\,\mathrm{FAs\ with\ one\ double\ bond}) + (2 \times \Sigma\,\mathrm{FAs\ with\ two\ double\ bonds}) + (3 \times \Sigma\,\mathrm{FAs\ with\ three\ double\ bonds}) + (4 \times \mathrm{x}\Sigma\,\mathrm{FAs\ with\ four\ double\ bonds})))/100$$

$$\mathrm{IA} = (\mathrm{C12} + 4 \times \mathrm{C14:0} + \mathrm{C16:0})/[\mathrm{MUFA} + \Sigma(\mathrm{n}{-}6) + \Sigma(\mathrm{n}{-}3)]$$

$$\mathrm{TI} = (\mathrm{C14:0} + \mathrm{C16:0} + \mathrm{C18:0})/[0.5 \times \mathrm{MUFA} + 0.5 \times (\mathrm{n}{-}6) + 3 \times (\mathrm{n}{-}3) + (\mathrm{n}{-}3)/(\mathrm{n}{-}6)]$$

2.6. Statistical analysis

Due to the lack of normality and homogeneity, Kruskal-Wallis non-parametric tests followed by Dunn's pairwise comparisons tests were employed to test for significant differences among sample groups (treatments type, dose and timepoints). Once a statistically significant result was found, Dunn's Test was performed to analyse pairwise comparisons between each independent group. Pairwise comparisons were performed for all comparisons possible. Spearman's correlations were also executed to test for significance between zinc concentrations in water and MDA concentrations as well as zinc found within animal tissue. Significance was set at $p < 0.05$. These analyses were all executed with the R Studio software v. 1.3.1093 (The RStudio Team).

Primer 6 software (Clarke and Gorley, 2006) was used to carry out multivariate statistical analyses using non-parametric multivariate analysis packages. The resemblance matrix of fatty acid concentrations (based on Euclidean distances) was analysed using SIMPER (Similarity Percentage package in Primer 6 software), to disclose the effects of each of the analysed variables in the sample grouping (Clarke and Gorley, 2006). Canonical Analysis of Principal coordinates (CAP) was used to generate statistical multivariate models based in the elemental concentrations, and to classify and separate the different geographical origin groups. This multivariate approach is insensitive to heterogeneous data and frequently used to compare different sample groups using the intrinsic characteristics (elemental concentrations) of each group (Cruz de Carvalho et al., 2020; Duarte et al., 2020). Chord diagram was performed using the average square distance (d^2) between sample groups obtained from the SIMPER analysis and plotted using the *circlize* package in R.

3. Results

3.1. Nanoparticle characterization

The zeta potential of the Zn nanoparticle determined by DLSS was found to be −3.6 ± 1.2 mV. Zinc nanoparticle size distribution could not be determined with DLSS due to agglomeration of the particles. However, electron micrograph confirmed size distribution as indicated by the

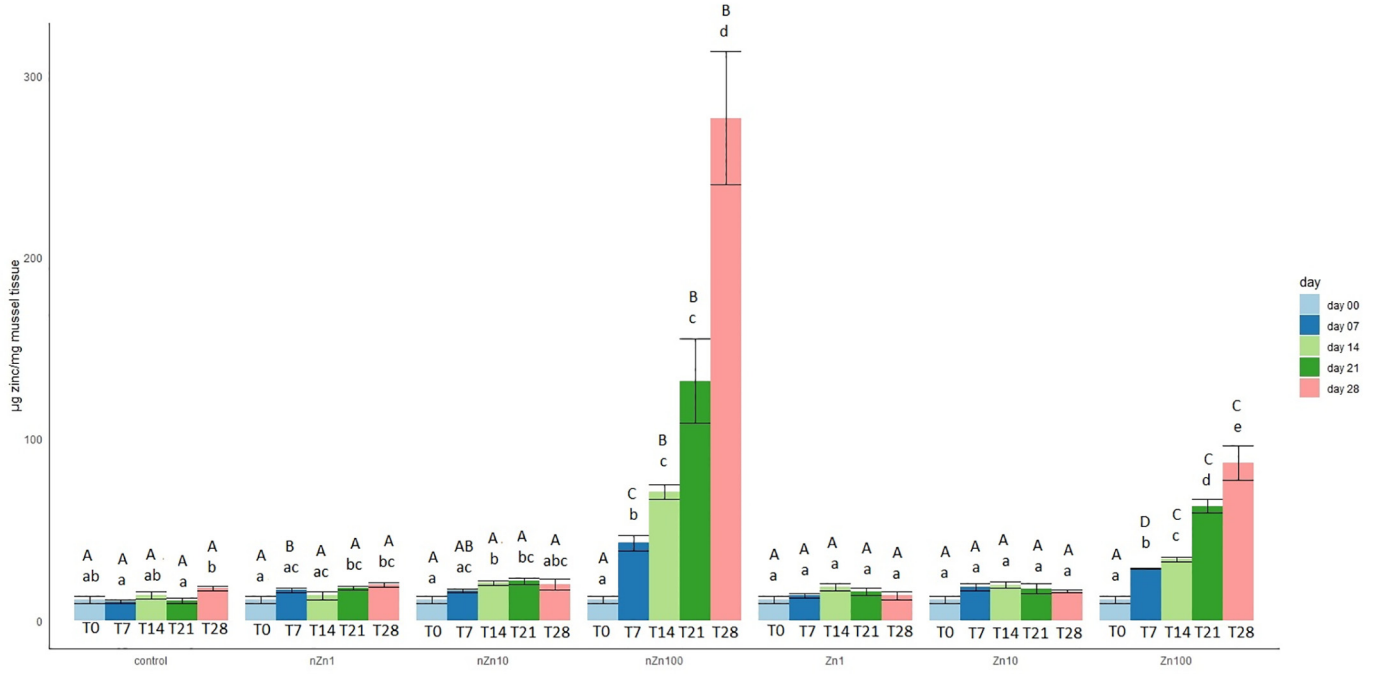

Fig. 1. Zinc concentration in mussel mantle edge exposed to zinc (Zn) and nano-zinc (nZn) (0, 1, 10 and 100 μg L^{-1}) for day 0, day 7, day 14, day 21 or day 28 (N = 175). Lowercase letters denote significant differences (p-value < 0.05) between different days, within the same experimental treatment. Uppercase letters denote significant differences (p-value < 0.05) within a specific day of the experiment, but between different treatments. Values correspond to average values ± standard error, n = 5.

Table I

Pairwise comparisons matrix regarding zinc concentration in mussel mantle edge exposed to zinc (Zn) and nano-zinc (nZn) (0, 1, 10 and 100 μg L^{-1}) for day 0, day 7, day 14, day 21 or day 28 (N = 175). Orange cells denote significant differences (*p*-value < 0.05) between different treatments, quantities or days of exposure.

Treatment			Control					nZn														Zn																	
	Concentration (ug/L)							1					10					100					1					10					100					
		Day	0	7	14	21	28	0	7	14	21	28	0	7	14	21	28	0	7	14	21	28	0	7	14	21	28	0	7	14	21	28	0	7	14	21	28	0	7	14	21	28
Control		0		0.77	0.71	0.89	0.18	1.00	0.27	0.93	0.07	0.04	1.00	0.62	0.03	0.04	0.34	1.00	0.03	0.01	0.00	0.00	1.00	0.87	0.23	0.31	0.60	1.00	0.23	0.09	0.26	0.17	1.00	0.02	0.00	0.00	0.00
		7			0.06	0.41	0.02	0.73	0.01	0.32	0.02	0.02	0.92	0.04	0.04	0.01	0.86	0.64	0.01	0.01	0.00	0.00	0.94	0.35	0.04	0.50	0.57	0.70	0.04	0.03	0.46	0.04	0.71	0.01	0.00	0.00	0.00
		14				0.81	0.78	0.99	0.59	0.99	0.46	0.98	0.85	0.83	0.34	0.99	0.79	0.61	0.02	0.02	0.01	0.01	0.33	0.25	0.57	0.10	0.42	0.73	0.77	0.46	0.76	0.84	0.88	0.08	0.00	0.00	0.00
		21					0.49	0.43	0.67	0.86	0.64	0.02	0.42	0.67	0.04	0.02	0.79	0.47	0.01	0.02	0.00	0.00	0.54	0.72	0.95	0.24	0.77	0.90	0.28	0.98	0.79	0.40	0.71	0.00	0.00	0.03	0.00
		28						0.35	0.70	0.32	0.76	0.73	0.41	0.54	0.43	0.83	0.39	0.90	0.01	0.01	0.00	0.01	0.96	0.33	0.75	0.32	0.46	0.55	0.36	0.45	0.54	0.46	0.42	0.02	0.00	0.00	0.01
nZn	1	0							0.27	0.93	0.07	0.04	1.00	0.62	0.03	0.04	0.34	1.00	0.03	0.01	0.00	0.00	1.00	0.87	0.23	0.31	0.60	1.00	0.23	0.09	0.26	0.17	1.00	0.02	0.00	0.00	0.00
		7								0.35	0.36	0.58	0.42	0.67	0.80	0.65	0.72	0.56	0.01	0.01	0.01	0.00	0.23	0.38	0.52	0.93	0.67	0.28	0.27	0.68	0.91	0.46	0.57	0.00	0.04	0.03	0.01
		14									0.25	0.53	0.84	0.80	0.47	0.33	0.16	0.71	0.01	0.01	0.00	0.00	0.91	0.53	0.41	0.52	0.64	0.84	0.68	0.84	0.74	0.15	0.65	0.00	0.04	0.01	0.00
		21										0.17	0.99	0.34	0.74	0.42	0.78	0.73	0.01	0.01	0.00	0.01	0.96	0.07	0.32	0.63	0.52	0.31	0.32	0.78	0.72	0.52	0.89	0.00	0.03	0.02	0.01
		28											0.01	0.20	0.40	0.49	0.47	0.02	0.01	0.02	0.00	0.01	0.03	0.05	0.59	0.42	0.78	0.04	0.43	0.79	0.79	0.28	0.71	0.00	0.02	0.02	0.00
	10	0												0.62	0.03	0.04	0.34	1.00	0.03	0.01	0.00	0.00	1.00	0.87	0.23	0.31	0.60	1.00	0.23	0.09	0.26	0.17	1.00	0.02	0.00	0.00	0.00
		7													0.06	0.07	0.24	0.45	0.02	0.02	0.00	0.01	0.31	0.68	0.52	0.37	0.23	0.52	0.59	0.76	0.42	0.29	0.67	0.00	0.02	0.02	0.01
		14														0.23	0.34	0.03	0.01	0.01	0.00	0.01	0.03	0.04	0.39	0.14	0.31	0.02	0.57	0.45	0.90	0.05	0.03	0.00	0.02	0.02	0.00
		21															0.97	0.04	0.01	0.03	0.01	0.00	0.03	0.05	0.57	0.35	0.11	0.02	0.62	0.43	0.71	0.06	0.01	0.00	0.03	0.01	0.01
		28																0.35	0.02	0.02	0.00	0.00	0.32	0.65	0.61	0.64	0.48	0.53	0.34	0.49	0.35	0.48	0.54	0.00	0.02	0.02	0.01
	100	0																	0.03	0.01	0.01	0.00	1.00	0.87	0.63	0.61	0.50	1.00	0.73	0.59	0.76	0.87	1.00	0.00	0.02	0.02	0.00
		7																		0.02	0.01	0.01	0.00	0.00	0.00	0.00	0.00	0.00	0.00	0.01	0.00	0.01	0.01	0.01	0.24	0.02	0.00
		14																			0.05	0.00	0.00	0.01	0.00	0.01	0.01	0.00	0.01	0.01	0.01	0.01	0.01	0.01	0.65	0.78
		21																				0.01	0.01	0.00	0.01	0.00	0.01	0.00	0.01	0.01	0.01	0.01	0.00	0.01	0.01	0.01	0.25
		28																					0.01	0.00	0.00	0.00	0.00	0.00	0.00	0.01	0.00	0.00	0.00	0.01	0.00	0.01	0.01
Zn	1	0																						0.87	0.23	0.31	0.60	1.00	0.23	0.09	0.26	0.17	1.00	0.02	0.00	0.00	0.00
		7																							0.14	0.35	0.10	0.59	0.47	0.12	0.61	0.48	0.67	0.01	0.01	0.00	0.00
		14																								0.78	0.76	0.41	0.61	0.51	0.66	0.74	0.38	0.02	0.02	0.01	0.00
		21																									0.29	0.35	0.48	0.57	0.36	0.72	0.32	0.01	0.01	0.01	0.00
		28																										0.59	0.41	0.43	0.54	0.59	0.44	0.02	0.01	0.00	0.00
	10	0																											0.23	0.09	0.26	0.17	1.00	0.02	0.00	0.00	0.00
		7																												0.71	0.86	0.33	0.14	0.04	0.03	0.01	0.00
		14																													0.72	0.31	0.13	0.05	0.03	0.01	0.00
		21																														0.30	0.05	0.04	0.03	0.01	0.00
		28																															0.29	0.01	0.00	0.00	0.00
	100	0																																0.02	0.00	0.00	0.00
		7																																	0.11	0.03	0.00
		14																																		0.26	0.03
		21																																			0.11
		28																																			

supplier (Suppl. Fig. S1A–D). Particle elemental composition and X-ray fluorescence spectra was obtained from the ZnO nanoparticles in seawater by TXRF as abovementioned (S2 PICOFOX, Bruker, Germany) (Suppl. Fig. S1E). X-ray fluorescence spectrum analysis revealed high amounts of Zn in ZnO nanoparticles suspension as well as of other minor elements, derived from the seawater composition.

3.2. Zinc analysis and quantification

Results for zinc concentrations in mussel mantle edge (Fig. 1) indicate that statistical differences are due to time of exposure ($\chi^2 = 56.4$, $p < 0.05$), particle form ($\chi^2 = 18.8$, $p < 0.05$), and concentration of the metal ($\chi^2 = 58$, $p < 0.05$). The matrix generated by Dunn's pairwise comparisons (Table I) was concurrent with these results as well: When looking at comparisons between all days, treatments and concentrations case-by-case, all the results from the control treatment were clearly significantly different from results pertaining to zinc treatments (control results were only occasionally statistically different at 1 and 10 μg $L^{-1}$of zinc treatments, but completely statistically different of all results of zinc treatments at 100 μg L^{-1}), and both zinc treatments had often significantly different results between each other at 100 μg L^{-1}, but when comparing the lowest two concentrations (1 and 10 μg L^{-1}) of both zinc forms directly against each other this was rarely the case. Regardless of treatment, the highest concentrations were always discernibly different from the lowest concentrations. Finally, in all zinc treatments time was also a significant factor of accumulation, although this was almost only obvious in the highest concentrated zinc treatments. As is, the longer and more concentrated the metal, the higher the accumulation, and nano-zinc accumulated to higher concentrations than ionic zinc.

When comparing to day zero, accumulation was first detected 21 days after of exposure for 1 μg L^{-1} nano-zinc, 14 days for 10 μg L^{-1} nano-zinc, and 7 days of treatment for 100 μg L^{-1} nano-zinc and for 100 μg L^{-1} ionic zinc. Lower concentrations of ionic zinc revealed no significant accumulation of this element. Nano-zinc at the two lowest concentrations at the most lead to a rise compared to control between 45 and 80%, however this was greatly surpassed at the highest concentration (rises of 281% at day 7, 545% at day 14, 1090% at day 21 and 2418% on the 28th day). Ionic zinc at the highest concentration comparatively to the same concentration on nano-zinc was not quite as high in its rise, but compared to control, on day 7 it rose 155%, on day 14 it rose 236%, on the 21st day it rose 473% and on the last day it rose 691%.

Spearman's correlations between zinc found within the mantle edge and the zinc concentration used in the experiment were significant ($p < 0.05$) for nano-zinc at day 7, 14, 21 and 28 of the experiment (Spearman's ρ = 0.861, 0.814, 0.915 and 0.651, respectively) and ionic zinc at day 7, 14, 21 and 28 of the experiment (Spearman's ρ = 0.861, 0.760, 0.814 and 0.504, respectively).

3.3. Lipid peroxidation

Results for the concentrations of lipid peroxidation products (Fig. 2) revealed that these were significantly dependent on the metal concentration ($\chi^2 = 78.6$, $p < 0.05$) and time ($\chi^2 = 63.7$, $p < 0.05$). There were also statistical differences between control and treatments ($\chi^2 = 42.1$, $p < 0.05$), but not between the two zinc forms tested. According to the matrix generate with Dunn's test (Table II), indeed if the concentration and day were the same, there were very few instances where both zinc treatments were significantly different from each other, however, the opposite scenario was observed when either treatment was compared to control. Furthermore, we saw that concentration was a very significant contributor for statistical differences in many treatments and days, once again, especially at the highest zinc concentration compared to the two lowest. The contribution of time as a factor for our results is also observable throughout the matrix, except for the highest concentrations where there are marked differences between all days, the lowest concentrations only exhibit significant differences between day 0 compared to all other days. In sum, the higher the concentration and time of exposure, the more MDA was accumulated.

Significant increases of lipid peroxidation products were detectable 7 days after the beginning of the exposure to the higher concentrations tested of both nano- and ionic zinc. A similar tendency was also observed for the lowest concentrations of zinc. MDA levels between control and treatments rose between 46 and 115%. At the highest concentration of

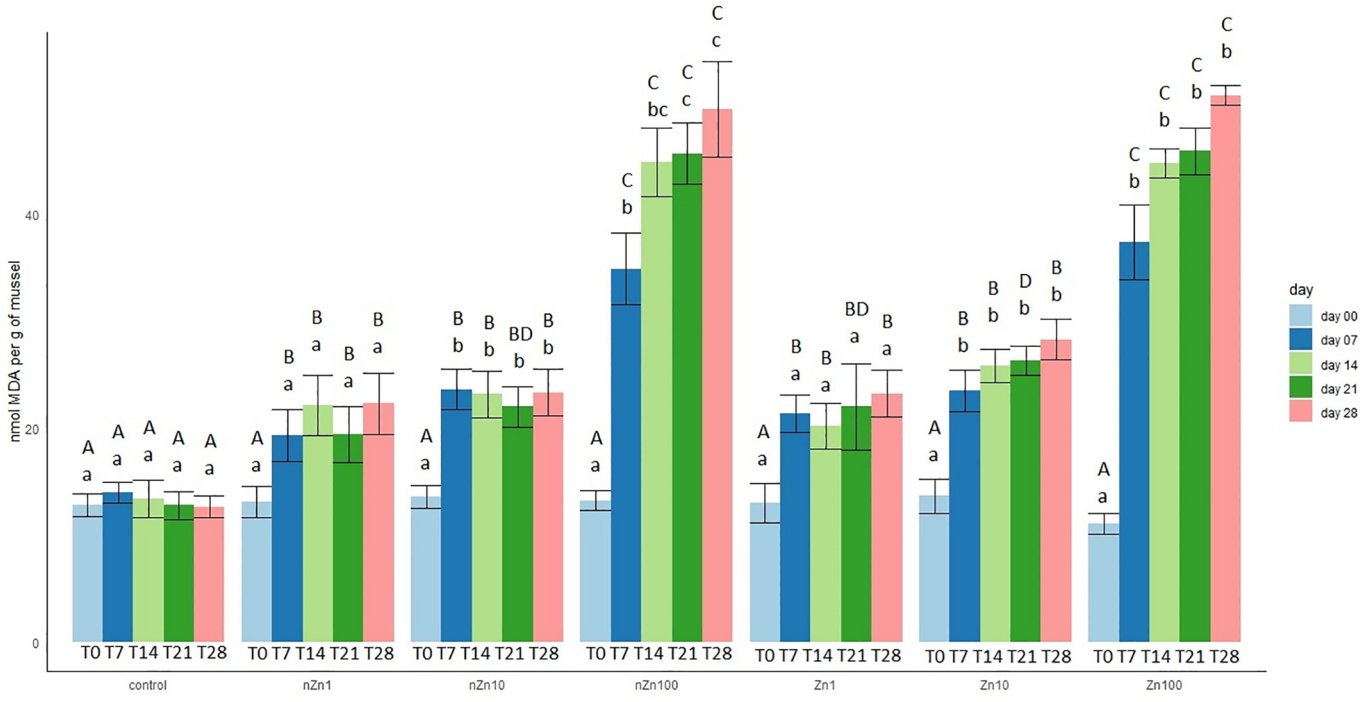

Fig. 2. Lipid peroxidation products concentration in mussel mantle edge exposed to zinc (Zn) and nano-zinc (nZn) (0, 1, 10 and 100 μg L^{-1}) for day 0, day 7, day 14, day 21 or day 28 (N = 210). Lowercase letters denote significant differences (p-value < 0.05) between different days, within the same experimental treatment. Uppercase letters denote significant differences (p-value < 0.05) within a specific day of the experiment, but between different treatments. Values correspond to average ± standard error, n = 6.

Table II

Pairwise comparisons matrix regarding lipid peroxidation products concentration in mussel mantle edge exposed to zinc (Zn) and nano-zinc (nZn) (0, 1, 10 and 100 μg L^{-1}) for day 0, day 7, day 14, day 21 or day 28 (N = 210). Orange cells denote significant differences (p-value < 0.05) between different treatments, quantities or days of exposure.

Treatment			Control					nZn														Zn																
	nmol MDA/g mussel tissue							1					10					100					1					10					100				
		day	0	7	14	21	28	0	7	14	21	28	0	7	14	21	28	0	7	14	21	28	0	7	14	21	28	0	7	14	21	28	0	7	14	21	28
Control		0		0.48	0.76	0.96	0.89	0.66	0.23	0.06	0.27	0.27	0.73	0.02	0.04	0.05	0.03	0.82	0.01	0.00	0.00	0.00	0.83	0.05	0.11	0.41	0.03	0.69	0.05	0.02	0.00	0.00	0.58	0.02	0.00	0.00	0.00
		7			0.46	0.61	0.57	0.44	0.78	0.30	0.73	0.23	0.85	0.03	0.03	0.04	0.03	0.89	0.01	0.00	0.00	0.00	0.71	0.04	0.15	0.30	0.02	0.53	0.03	0.00	0.00	0.00	0.31	0.01	0.00	0.00	0.00
		14				0.75	0.51	0.62	0.28	0.14	0.24	0.18	0.39	0.03	0.05	0.07	0.04	0.68	0.01	0.00	0.00	0.00	0.85	0.16	0.21	0.40	0.05	0.77	0.04	0.01	0.00	0.00	0.46	0.00	0.01	0.00	0.00
		21					0.72	0.84	0.28	0.17	0.26	0.17	0.63	0.01	0.02	0.04	0.02	0.46	0.01	0.00	0.00	0.00	0.68	0.04	0.12	0.40	0.02	0.46	0.04	0.04	0.02	0.00	0.30	0.02	0.00	0.00	0.00
		28						0.70	0.13	0.05	0.21	0.04	0.71	0.02	0.03	0.03	0.02	0.81	0.01	0.01	0.00	0.00	0.55	0.04	0.06	0.10	0.03	0.59	0.03	0.03	0.02	0.00	0.83	0.01	0.00	0.01	0.00
nZn	1	0							0.29	0.18	0.26	0.18	0.65	0.01	0.03	0.04	0.02	0.48	0.01	0.01	0.00	0.00	0.69	0.04	0.13	0.41	0.02	0.48	0.04	0.04	0.02	0.01	0.30	0.02	0.00	0.01	0.00
		7								0.69	0.85	0.66	0.17	0.20	0.32	0.91	0.60	0.22	0.03	0.00	0.00	0.00	0.47	0.62	0.50	0.42	0.46	0.53	0.48	0.23	0.21	0.18	0.05	0.03	0.00	0.00	0.00
		14									0.65	0.96	0.07	0.78	0.62	0.72	0.76	0.08	0.23	0.03	0.02	0.01	0.19	0.42	0.60	0.95	0.76	0.28	0.73	0.65	0.58	0.46	0.04	0.07	0.02	0.03	0.01
		21										0.75	0.25	0.65	0.46	0.48	0.35	0.51	0.04	0.02	0.00	0.00	0.38	0.61	1.00	0.61	0.22	0.43	0.66	0.35	0.28	0.22	0.19	0.04	0.01	0.00	0.00
		28											0.16	0.27	0.26	0.28	0.79	0.08	0.25	0.02	0.02	0.00	0.28	0.59	0.79	0.74	0.81	0.29	0.57	0.54	0.42	0.22	0.04	0.88	0.04	0.01	0.00
	10	0												0.03	0.03	0.04	0.03	0.89	0.01	0.00	0.00	0.00	0.71	0.04	0.15	0.30	0.02	0.53	0.03	0.00	0.00	0.00	0.31	0.01	0.00	0.00	0.00
		7													0.89	0.86	0.82	0.03	0.15	0.01	0.01	0.00	0.04	0.42	0.39	0.26	0.69	0.02	0.99	0.37	0.26	0.40	0.02	0.05	0.02	0.02	0.00
		14														0.76	0.89	0.04	0.16	0.01	0.01	0.00	0.04	0.63	0.40	0.33	0.69	0.04	0.99	0.37	0.26	0.47	0.02	0.05	0.01	0.02	0.00
		21															0.70	0.03	0.05	0.04	0.01	0.00	0.09	0.75	0.60	0.44	0.59	0.11	0.89	0.70	0.52	0.88	0.03	0.03	0.02	0.02	0.00
		28																0.04	0.16	0.01	0.01	0.00	0.04	0.63	0.40	0.33	0.69	0.04	0.99	0.37	0.26	0.47	0.02	0.05	0.01	0.02	0.00
	100	0																	0.01	0.00	0.00	0.00	0.83	0.05	0.11	0.41	0.03	0.69	0.05	0.02	0.00	0.00	0.58	0.02	0.00	0.00	0.00
		7																		0.46	0.35	0.23	0.00	0.04	0.03	0.35	0.14	0.00	0.17	0.26	0.27	0.32	0.00	0.62	0.10	0.08	0.03
		14																			0.85	0.48	0.00	0.01	0.01	0.02	0.02	0.00	0.02	0.02	0.02	0.03	0.00	0.27	0.39	0.57	0.28
		21																				0.44	0.00	0.01	0.01	0.02	0.02	0.00	0.02	0.03	0.03	0.04	0.00	0.29	0.40	0.59	0.29
		28																					0.00	0.01	0.01	0.02	0.02	0.00	0.02	0.03	0.03	0.04	0.00	0.29	0.19	0.54	0.09
Zn	1	0																						0.16	0.21	0.40	0.05	0.77	0.04	0.01	0.00	0.00	0.46	0.00	0.01	0.00	0.00
		7																							0.12	0.40	0.02	0.46	0.04	0.04	0.02	0.00	0.30	0.02	0.00	0.00	0.00
		14																								0.62	0.43	0.13	0.21	0.17	0.20	0.50	0.03	0.04	0.00	0.01	0.00
		21																									0.80	0.42	0.38	0.61	0.34	0.48	0.19	0.67	0.02	0.01	0.00
		28																										0.04	0.99	0.37	0.26	0.47	0.02	0.05	0.01	0.02	0.00
	10	0																											0.04	0.01	0.00	0.00	0.43	0.00	0.01	0.00	0.00
		7																												0.23	0.21	0.18	0.05	0.03	0.00	0.00	0.00
		14																													0.81	0.67	0.02	0.07	0.03	0.03	0.01
		21																														0.66	0.02	0.06	0.02	0.03	0.01
		28																															0.02	0.26	0.04	0.04	0.02
	100	0																																0.00	0.00	0.00	0.00
		7																																	0.18	0.07	0.03
		14																																		0.70	0.04
		21																																			0.12
		28																																			

nano-zinc we saw rises of 169% at day 7, 246% at day 14, 253% at day 21 and finally 285% on the 28th day. Ionic zinc at the highest concentration was comparatively to the same concentration on nano-zinc, and on day 7 it rose 185%, on day 14 it rose 246%, on the 21st day it rose 253% and on the last day it rose 292% compared to control.

Spearman's correlations between MDA concentrations found within the mantle edge analysed and the zinc concentration supplied to the medium at the beginning of the experiment were significant ($p < 0.05$) within the treatments of nano-zinc at day 7, 14, 21 and 28 of the experiment (Spearman's $\rho = 0.76$, 0.682, 0.787 and 0.721, respectively) and likewise significant concerning the treatments of ionic zinc at day 7, 14, 21 and 28 of the experiment (Spearman's $\rho = 0.748$, 0.839, 0.8 and 0.826, respectively).

3.4. Fatty acid profiles

Lipid peroxidation products accumulations were highest at the end of the exposure period (28 days) at 10 and 100 μg L^{-1} in both zinc forms, and thus the fatty acid profiles of these individuals were analysed in the same exposure period and concentrations.

Fatty acid (FA) profiles are displayed in Fig. 3. In the mantle edge the most abundant fatty acids are palmitic acid (PA, C16:0), oleic acid (OA, C18:1 n-9), eicosapentaenoic acid (EPA, C20:5 n-3) and docosahexaenoic acid (DHA, C22:6 n-3). The percentage of C16:0 was slightly lower in animals exposed to 10 μg L^{-1} of nano-zinc but much higher in samples treated with 100 μg L^{-1} of this metal form compared to controls. A similar trend was observed in response to nano-zinc but with smaller variations. Regarding the mono-unsaturated C18:1 n-9, zinc at 100 μg L^{-1} caused significant increase in this FA, while small decreases were observed in response to the remaining treatment. The EPA percentages in metal-exposed mussels were significantly lower than those found in controls, especially when ionic zinc was used. In contrast, there were no differences between treatments for the other omega 3 LC-PUFA, DHA.

Other significant and diverse differences between control and treatments were observed in several other FA, especially when compared to the highest concentration of both forms of zinc:

Specifically, all concentrations of nano-zinc caused significant increases in myristic acid (C14:0), octadecatetraenoic acid (C18-4 n-3) and eicosadienoic acid (C20:2); while increases exclusive to the lowest concentration were observed for cis-vaccenic acid (C18:1 n-7), linoleic acid (C18:2 n-6), and for the higher concentration in ginkgolic acid (C15:1), cis-7-hexadecenoic acid (C16:1 n-9), hexadecatrienoic acid (C16:3) and hexadecatetraenoic acid (C16:4). However, 100 μg L^{-1} of this zinc form also caused decreases compared to controls, such as in myristoleic acid (C14:1), margaric acid (C17:0), stearic acid (C18:0), C18:2 n-6, linolenic acid (C18:3 n-3) and arachidonic acid (C20:4 n-6).

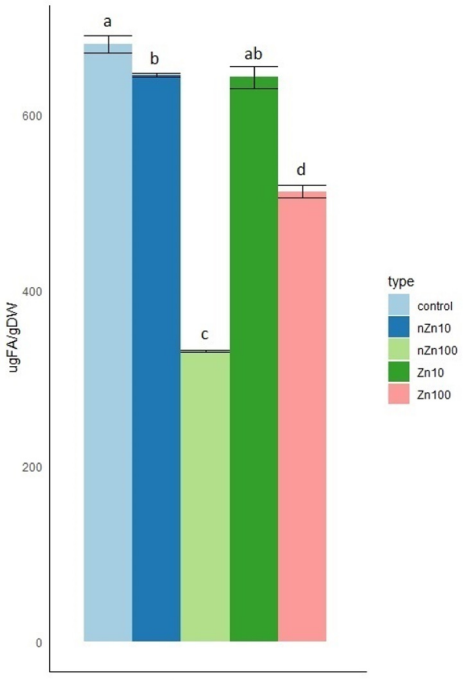

Fig. 4a. Total fatty acid content of mussel mantle edge (expressed as micrograms of fatty acid per gram of mussel tissue dry weight) exposed to zinc (Zn) and nano-zinc (nZn) (10 and 100 μg L^{-1}) for 28 days. Lowercase letters denote significant differences (p-value < 0.05) between different treatments. Values correspond to average ± standard error, n = 3.

In the case of ionic zinc, fluctuations in FA concentrations were also recorded: At its highest concentration, significant decreases were registered for C15:1 and C16:1 n-9, and significant increases for C17:0, C18:0, C18:1 n-7, C18:2 n-6, C18:3 n-3 and C18:4 n-3. Meanwhile 10 μg L^{-1} of this metal caused minor but significant increases of C18:2 n-6 and C20:2.

Concerning total FA content on the analysed mussel tissues, a significant decrease ($p < 0.05$) was observed in cells exposed to ionic zinc and nano-zinc at the highest concentrations (100 μg L^{-1}) and nano-zinc at 10 μg L^{-1} (Fig. 4a). The animals treated with the higher nano-zinc concentration had the lower FA content.

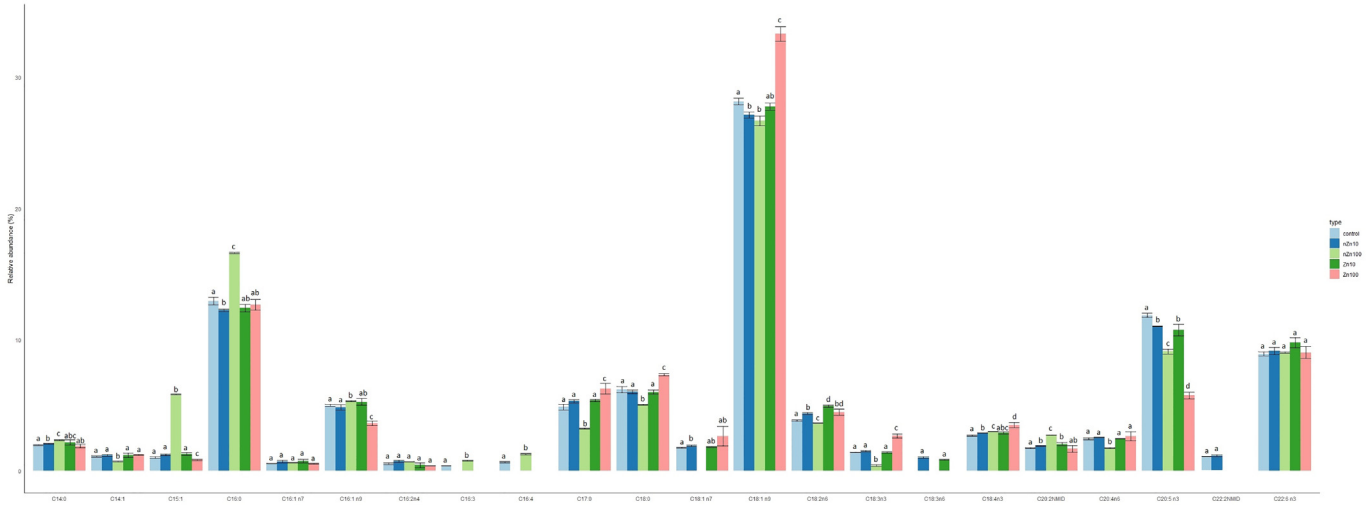

Fig. 3. Fatty acid profiles of mussel mantle edge exposed to zinc (Zn) and nano-zinc (nZn) (10 and 100 μg L^{-1}) for 28 days. Lowercase letters denote significant differences (p-value < 0.05) between different treatments. Values correspond to average ± standard error, n = 3.

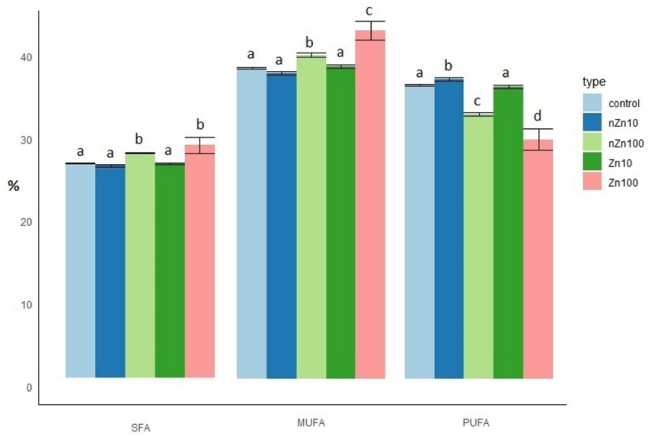

Fig. 4b. Percentages of saturated fatty acids (SFA), monosaturated fatty acids (MUFA) and polyunsaturated fatty acids (PUFA) exposed to zinc (Zn) and nano-zinc (nZn) (10 and 100 μg L^{-1}) plus the control treatment. Lowercase letters denote significant differences (p-value < 0.05) between different treatments. Values correspond to average ± standard error, n = 3.

In regard to FA unsaturation classes (Fig. 4b), the relative amounts of saturated FA (SFA) increased significantly in the response to the highest concentrations of both forms of zinc. The same was observed for monounsaturated FA (MUFA), but more pronounced for 100 μg L^{-1} of nano-zinc. Mussels submitted to the higher metal concentrations, especially in the ionic form, had significant lower contents of PUFA compared to controls, whereas 10 μg L^{-1} of nano-zinc caused a slight increase of FA with two or more double bonds.

The above-mentioned changes in the fatty acid profiles of mussels exposed to metals impacted several indexes related to membrane fluidity and nutritional value of the animals: The double bond index (DBI) as well as the ratios PUFA/SFA and UFA/SFA (Fig. 4c) decreased in all animals exposed to the highest concentrations of both zinc forms, although there was a slight increase in the PUFA/SFA ratio in the case of nano-zinc at 10 μg L^{-1}; The ratios of n-6/n-3 FA were higher in metal-exposed animals in comparison to controls but remained unchanged in response to 100 μg L^{-1} nano-zinc; Finally, regarding the index of thrombogenicity (IT) 100 μg L^{-1} of both nano- and ionic zinc resulted in higher values compared to controls. The same was also observed in response to that concentration of nano-zinc but not to its ionic counterpart for the index of atherogenicity (IA).

Aiming to disentangle the potential of fatty acid profiles as biomarkers for zinc exposure (including the metal form and concentration), the fatty acid concentrations was analysed as a profile in a multivariate approach. The canonical analysis of principal coordinates (CAP) (Fig. 5) yielded a 100% classification efficiency, indicating that the fatty acid profiles of the mussel exposed for 28 days to different zinc forms and concentrations are efficient biomarkers of the exposure conditions and its biochemical effects. This analysis showed a clear separation of treatments, having as basis their FA profile. Through the SIMPER analysis it was possible to identify the dissimilarity between treatments (Fig. 6). Surprisingly, the highest dissimilarity was not verified between the control group and any of the zinc treatments, but between the two zinc treatments at the 100 μg L^{-1} concentration (d^2 = 138.19). On the other hand, the lower dissimilarity was observed between the fatty acid profiles of the individuals exposes to the two zinc forms at 10 μg L^{-1} (d^2 = 5.17). Focusing on the differences between the fatty acid profiles of the specimens exposed to 10 and 100 μg L^{-1}, a high average square distance value as observable for both ionic (d^2 = 73.37) and nano-zinc (d^2 = 62.76) treatments. Comparing the two highest dose treatments in both tested forms it could be observed that the highest dissimilarity in terms of fatty acid profiles was assessed for the individuals exposed to ionic zinc (d^2 = 80.97), when compared to the organisms subjected to nano-zinc (d^2 = 59.69).

4. Discussion

This study has shown that the longer the exposure and the higher the concentration of the contaminant zinc, the higher were the rates of metal accumulation, oxidative stress and fatty acid alterations, in the mussel *Mytilus galloprovincialis*. For the first time this issue was investigated by comparing the effects of the exposure to zinc in its nano- and ionic form, revealing that the nanoparticulate form leads to much higher accumulation of the metal. This is a critical finding given the current increase in the production of nanoparticles by multiple industries. Alterations on the fatty acid profiles were found to lower the mussel quality as a food source for its predators, with potential effects cascading through food webs and ultimately reaching humans.

Additionally, a canonical analysis of principal coordinates of the fatty acid profiles showed a clear separation between the samples treated with the different concentrations of ionic and nano-zinc, revealing a high potential for its' use as a set of biomarkers of zinc exposure. Given the current

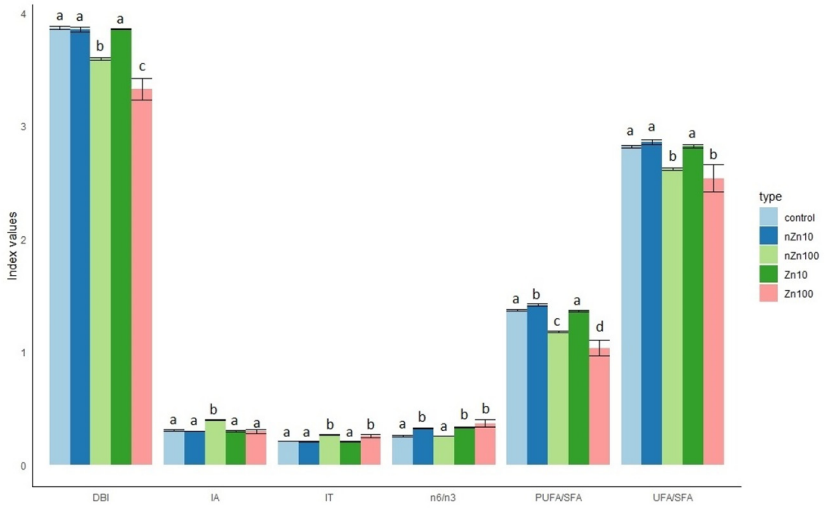

Fig. 4c. Fatty acid-derived indexes of mussel mantle edge exposed to zinc (Zn) and nano-zinc (nZn) (10 and 100 μg L^{-1}) for 28 days: Double bond index (DBI), index of atherogenicity (IA), index of thrombogenicity (IT), omega-6/omega-3 ratio (n6/n3), polyunsaturated to saturated fatty acids (PUFA/SFA) and unsaturated to saturated fatty acids (UFA/SFA). Lowercase letters denote significant differences (p-value < 0.05) between different treatments. Values correspond to average ± standard error, n = 3.

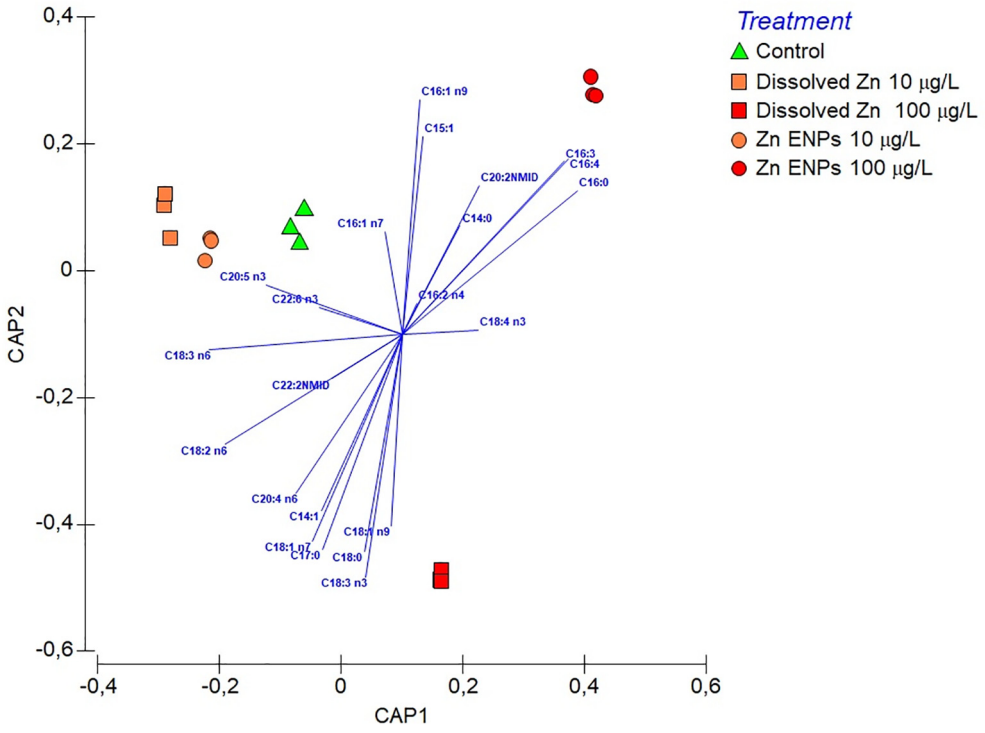

Fig. 5. Canonical analysis of principal (CAP) coordinates of *M. galloprovincialis* (N = 20) exposed to zinc (Zn) and nano-zinc (nZn) (10 and 100 μg L^{-1}) plus the control treatment (100% classification efficiency).

difficulties in assessing contamination by nano metal forms, this finding opens interesting avenues for future environmental monitoring.

4.1. Zinc accumulation in mussel tissue

Zinc accumulation in mussel tissue generally increased with increasing zinc external concentration and longer exposures times. In fact, the highest accumulation was verified at the highest concentration and time of exposure, even if occasionally at lower concentrations and exposure times significant differences were spotted. This trend had been observed before in other similar studies (e.g. Hanna et al., 2013) with *M. galloprovincialis*. However, we found that the rates of nano-zinc and ionic zinc uptake were also significantly different: there was a much higher accumulation of nano-zinc. So far only a few reports of comparable studies are available in the literature, for example, Li et al. (2018) tested $ZnSO_4$ accumulation versus ZnO NPs (0.01, 0.1, 1, 10, and 100 mg Zn/L and sampled on the 1st, 2nd, 3rd, 7th, 14th, 21st, and 28th day) but they observed an opposite trend, with ionic zinc inducing higher rates of accumulation – this may be explained by several reasons: the digestive gland was analysed instead of the muscle tissue analysed in our work; quantities of pollutant tested were much higher leading to higher expectable toxicity degrees; after 3 days of exposure to the highest concentrations a high mortality of the mussels was verified, which did not occur in our experiment; and the organism density per aquaria and volume of water was significantly different (25 mussels per 5 L aquaria in Li et al. (2018) versus 10 mussels per 12 L aquaria in our study). Differences from both studies can also arise from less obvious experimental differences, starting in the zinc nanoparticle tested, as its physic-chemical features have a critical role on its behaviour in the water medium.

4.2. Lipid peroxidation

Adverse effects occurred in the lipids of *M. galloprovincialis* mussels exposed to both zinc in ionic and NP forms: Lipid peroxidation products accumulation was proved dependent on time of exposure and concentration tested, once again with higher concentrations and exposure time to the contaminant being decisive factors in MDA accumulation. While there were a few instances where the form of the zinc particle was relevant, overall this was not an important factor. This form of toxicity has been seen before in *M. galloprovinciallis* in other studies in response to stress generated by the presence of heavy metals in the exposure media (e.g. Vlahogianni and Valavandis, 2007; Taze et al., 2016), and follows the same trends (exposure time and concentration-wise) although more often than not, this is a biomarker that is more easily detected in the haemolymph or digestive gland, as often muscle is considered a low-priority target for accumulation, and therefore other forms for toxicity, for metals (Duroudier et al., 2019). Furthermore, although the changes in MDA content were similar between both zinc forms used, nano-zinc caused a higher decrease in the total lipid content in agreement with the higher accumulation of this metal form in mussel mantle.

4.3. Fatty acids profile changes

The fatty acid (FA) profiles of mussels are subjected to various changes throughout their lifetime, due to changes in temperature, food availability and sources, development stage, phase of the reproductive cycle, etc. (Murphy et al., 2002; Lachance et al., 2008). This leads to complex relationships between the enzymes that control membrane lipid composition and reserves within the body, and multiple endogenous and exogenous stimuli that change the activity of these enzymes. In fact the mussel used in this study, *M. galloprovincialis*, has reportedly a FA composition that varies widely depending on latitude and the obtention of nutrients typical of specific geographical features (Ventrella et al., 2008). Nevertheless, the fatty acid profiles of the control animals reported in the present study agree with previous reports for this species (e.g. Freites et al., 2002; Prato et al., 2010; Dernekbaşı et al., 2015; Signa et al., 2015). However, the object of this study, the relationship between metal toxicity (nano or ionic) and changes in the fatty acid profile, is still severely understudied, and long-term consequences are difficult to ascertain. Moreover to our knowledge, no studies dealt with the specific conditions tested in our work.

For this study we chose to sample from the mantle edges, as these are the first body parts that come into contact with all sources of environmental stressors, and measuring the first point of contact with a stressor is essential

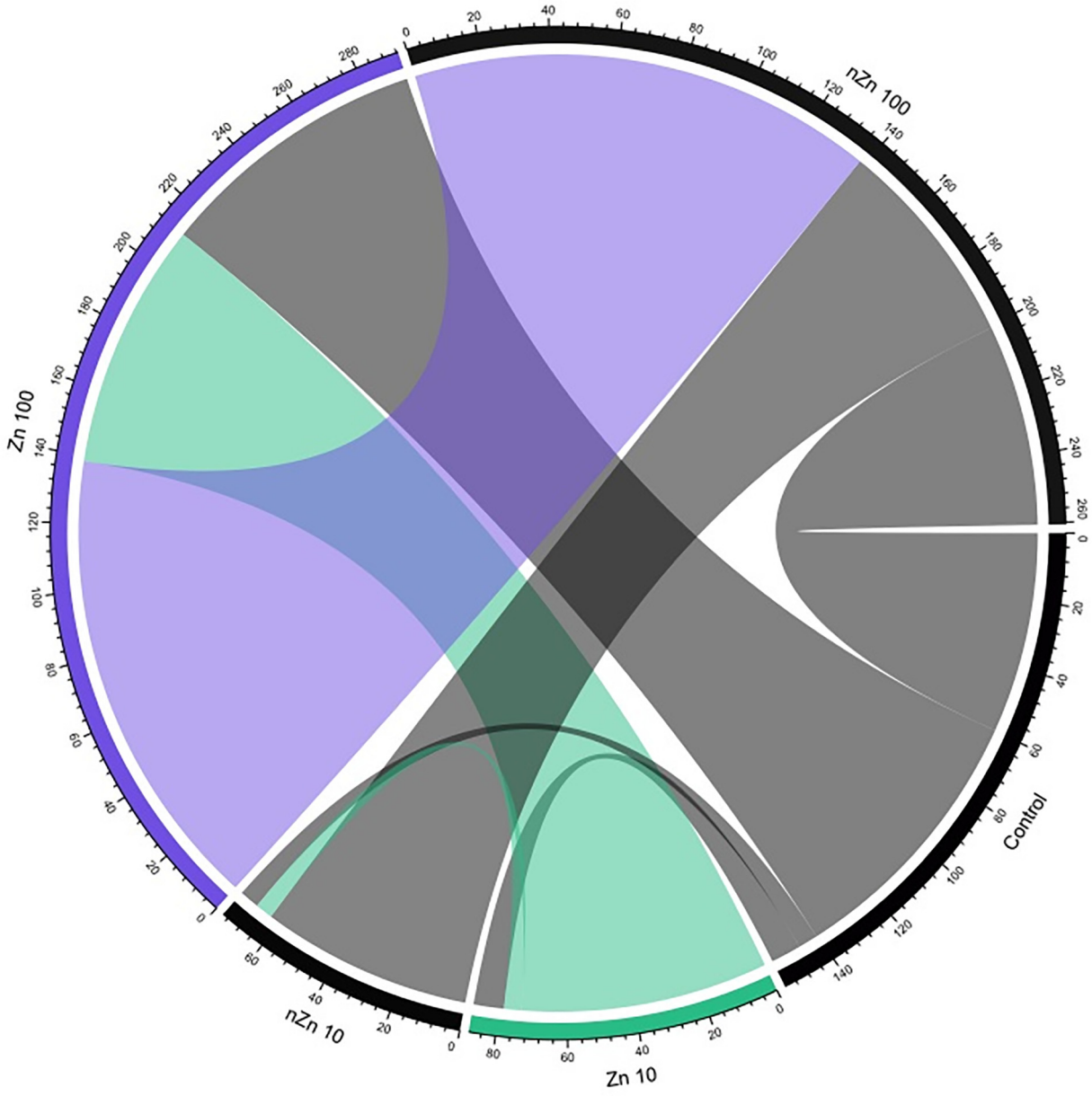

Fig. 6. Chord diagram having as basis the average square distance based in the SIMPER analysis between the groups of samples subjected to the different levels of zinc (Zn) and nano-zinc (nZn) (10 and 100 μg L^{-1}) plus the control treatment.

to understanding how an animal copes with this disturbance at first instance. Whatever the tissue used however, the cells that come into contact with stressors have their membranes subjected to alterations which often trigger an adaptative strategy, that can be translated in the alterations in the FA profile and under more severe stress conditions can cause cell membrane damage, revealed by the accumulation of lipid peroxidation products and decreases in the total lipid contents. As most bivalves respond to stress induced by metals by causing disturbances in lipid metabolism (Fokina et al., 2013), changes to the FA composition may be indicative of changes in the structure and fluidity of cell membranes, confirming the occurrence of pathological or compensatory alterations in lipid metabolism caused by contaminant exposure (Fokina et al., 2013).

4.3.1. Individual fatty acids

As a general rule, we saw that MUFA comprised the more abundant FAs in the mantle edge, followed by PUFA and SFA. The main contributor to MUFA quantities was C18:1 n-9 that also presented the highest proportions of all FA: oleic acid is an abundant FA in marine animals and was here shown to be affected by both zinc forms: At high quantities, ionic zinc increased (about 5%) the presence of this FA, but nano-zinc, although smaller, clearly a negative effect on this FA. This FA was followed by high quantities of C16:0, C20:5 n-3 and C22:6 n-3, while the remaining FA had only modicum quantities present, explaining the overall composition of saturation classes we subsequently observed.

The presence of FA of bacterial origin like C15:1, C17:0 and C18:1 n-7 can, to some degree, be traced back to the presence of vestigial amounts of bacteria (Parkes and Taylor, 1983). However, it has been verified that C18:1 n-7 can also be derived from chain elongation of the phytoplankton FA C16:1 n-7 (e.g. Graeve et al., 1997; Falk-Petersen et al., 2000; Kharlamenko et al., 2001). In any event, C17:0 and C18:1 n-7 were also affected negatively mainly by nano-zinc, which also had a negative effect on C18:0, estimated to have a structural-type function in marine invertebrates (Kaneda, 1967; Perry et al., 1979; Pazos et al., 1997; Labarta et al., 1999).

Other FA found include a well-known group of FA in marine molluscs that are biosynthesized de novo endogenously (Zhukova, 1991): the so-called non-methylene-interrupted dienoic fatty acids (NMID FA) such as

C20:2 and C22:2, which were detected in some of the organisms used in the present study, and are known to have functional and structural roles in the membranes (Kraffe et al., 2004) including enhancing protection from oxidation, and are found in considerable proportions in phospholipids of organs exposed to the external environment, including the mantle (Klingensmith, 1982). In fact, Barnathan (2009) stated that these FAs reduce susceptibility to peroxidation by ROS. Therefore, an increase in C20:2 content, such as the one observed in response to 100 μg L^{-1} nano-zinc, may be indicative of an increase in cell protective functions during stress.

Seeing as the mussels were fed a monodiet consisting of *P. tricornutum*, this diatom is the likeliest source of C16:1 n-7, C16:2 n-4, C16:3, C16:4, C18:3 n-3, C18:4 n-3 and C20:5 n-3 (Graeve et al., 1994; Feijão et al., 2020) detected in the sampled mussel tissue. EPA, docosahexaenoic acid (DHA, C22:6 n-3), and arachidonic acid (ARA, C20:4 n-6) are among the most important LC-PUFA available (Alkanani et al., 2007; Parrish, 2009) for bivalves, but these organisms may have limited or inexistent capacity for its synthesis, and environmental stresses may further hinder their capacity for the production and/or accumulation of these FAs (Fokina et al., 2013). Furthermore, both EPA and ARA FAs serve as precursors for eicosanoids (such as leukotrienes, prostaglandins, thromboxanes, etc.) which are vital to various physiological responses, including inflammatory, immunological, neural, reproductive and as a stress adaptor (DeCaterina and Basta, 2001), and since in our study both EPA and ARA were negatively affected by the presence of zinc, there is a high likelihood of this stressor having a high impact on the overall health state of the animal. Interestingly enough however, DHA suffered no effects during the experiments, which may be an indication of its importance: like EPA and AA, this FA does not come from the food our mussels ingested, and yet if its levels were maintained, which may be suggestive of the organism prioritizing somehow the continued production of DHA in situations of stress, as a survival mechanism. Lastly, EPA along with FAs like C14:0 and C16:0, can also be used as energy reserves for metabolic purposes, and usually a decline in their reserves can be telling that there was an increase in animals' metabolic rate related to stressors in their environment. While EPA quantities declined with rising zinc quantities, C16:0 saw a marked great rise in its quantities within the treatment of nano-zinc at 100 μg L^{-1}, but remaining zinc treatments had little effect. This may be explained by the fact that C16:0 likely also comes in significant quantities from the mussels' food source (microalgae monodiet), and when comparing its quantities in our results to those of Feijão et al. (2020) there was an obvious transfer of this SFA through the food chain, supporting the high concentrations present in the mussel tissues. This was also observed in previous works with mussels feeding on algal food sources (e.g. Prato et al., 2010).

4.3.2. Fatty acid groups

Both zinc forms lowered PUFA and increased SFA and MUFA. Membrane PUFA are essential components of membrane phospholipids and storage lipids, providing several key functions to living being's metabolism, including energy reserves and cell structural functions. When exposed to ROS these FA are prone to suffer peroxidation (Valko et al., 2005; Vlahogianni and Valavandis, 2007). Drops in PUFA levels (which happened for the highest concentrations of both zinc forms) may be associated with stress, including the type related to contaminant exposure, which leads to cytotocixity and membrane fluidity decline (Langdon and Waldock, 1981; Freites et al., 2002). According to our results, nano-zinc had a much higher impact on changes in the aforementioned unsaturated class than ionic zinc. While looking at individual FA proportions, the variations may not have seemed dramatic, but ultimately nano-zinc was generally deemed more harmful to mussels than ionic zinc. Even though at its lowest exposure concentration nano-zinc slightly promoted the accumulation of PUFAs, this did not translate into the individual accumulation of FAs that are widely known to improve vascular and neural health at a significant level, like EPA (Calder, 2015, 2018), in fact this FA had its abundance lowered by the presence of this concentration as well.

As such, zinc treatments particularly at their highest concentration resulted in a negative effect on PUFA/SFA and UFA/SFA rations, consequently also negatively influencing the DBI rates. A decrease in the number of double bonds inevitably affects membrane fluidity – the higher the number of double bonds, the higher the fluidity of the cell's membrane. This fluidity determines rotation and diffusion of proteins and other biomolecules within the cell membrane, thereby ultimately dictating how their functions may be modified (Gennis, 1989).

Likewise, in our study we saw an increase of the n-6/n-3 ratio, enhancing how zinc treatments have the potential for a clearly negative impact even when one considers mussels as potential option for a healthy diet: Mussels are part of a group of interest to several fishing industries that are looking into alternative means of production of n-3 long-chain PUFA, so the pressure on fish stocks can be alleviated (Monroig and Kabeya, 2018).

Similarly within the subject of human health, or even upper trophic level organism health, there were also marked changes in the indexes of atherogenicity (IA) and thrombogenicity (IT): while the first is related to the formations of plaques decrease in the levels of esterified fatty acid, cholesterol, and phospholipids, and hence thwarting the appearance of micro- and macro-coronary diseases, the second one is related to the propensity to form clots in blood vessels (Garaffo et al., 2011). A low ratio of IA and IT is therefore usually recommended by medical physicians. As an example, tuna serves as a reference animal for human consumption, due to its high nutritional value related to its fatty acid content: it has an IA of about 0.7 and an IT around 0.3 (Garaffo et al., 2011), therefore our results with the mussel *M. galloprovincialis* where all IA values remained below 0.4 and all IT values remained under 0.3 indicate that whatever the treatment, there seems to be no immediate danger to human health based on the zinc treatments we experimented with. Nevertheless, both zinc forms at their highest concentration increased IT significantly from its control values, while nano-zinc also significantly increased IA. However, the experiment lasted only 28 days at constant concentrations lower than those that can be found outside the laboratorial environment, beyond these specific conditions it is difficult to ascertain if mussels exposed to these contaminants for longer periods would remain unaffected.

5. Conclusion

This study was the first of its kind to demonstrate side-by-side comparisons of different forms of zinc and their effects on *M. galloprovincialis* biomarkers, including a direct comparison of its effects on the fatty acid profiles of this mussel.

Although the majority of this type of studies tend to evaluate stress in digestive glands and gills, the results here presented show that the fatty acid profiles of the mantle edge tissue showed to be a promising target tissue for biomarkers of exposure to zinc. This was not only true if we consider fatty acids as biomarkers of the zinc concentration used for exposure, but also for the metal form used. Analysing the fatty acid profile as a whole instead of each fatty acid individually proved not only to be an efficient set of biomarkers able to distinguish the dose and form of zinc to which the mussels were exposed, pointing out the utility of these profiles in ecotoxicology and nanotoxicology, but also indicating that zinc in different forms and concentrations present differential Adverse Outcome Pathways (AOPs) in mussels and therefore its modes of action need to be addressed more deeply.

Our results highlighted clear negative effects of zinc on the mussel *Mytilus galloprovincialis*, both under ionic and nanoparticulate forms, palpably dependent on exposure time and concentration. The concentrations tested in the present work are theoretically possible to achieve *in natura*, at least in some locations closer to effluent disposal, and as such the toxicity that was generated should be considered worrying, as there is a high possibility for negative effects in the marine trophic chains and also ultimately impacts on human health, especially considering how more and more the fisheries industries look for multiple sources of protein in the latest years.

In sum, the higher the concentration of the metallic stressor, and the longer the mussel is exposed to it, the more toxic effects are verified.

Moreover, the negative impacts observed in mussels exposed not only the ionic zinc form but also to its nanoparticle counterpart highlight the importance of analysing different forms of metals in toxicity tests. The increasing introduction of metal particles in the aquatic environment and the negative effects they might have in marine biota, including lipid peroxidation and fatty acid profile changes, can affect other organisms at higher trophic levels and ultimately have negative impacts on human health, highlights the considerable importance of these types of studies.

CRediT authorship contribution statement

Joana Roma: Software, Validation, Formal analysis, Investigation, Data curation, Writing – original draft, Visualization, Funding acquisition, Project administration. **Eduardo Feijão:** Investigation, Writing – review & editing. **Catarina Vinagre:** Conceptualization, Methodology, Resources, Writing – review & editing, Supervision, Funding acquisition. **Bernardo Duarte:** Conceptualization, Methodology, Software, Validation, Formal analysis, Resources, Writing – review & editing, Visualization, Supervision, Funding acquisition. **Ana Rita Matos:** Conceptualization, Methodology, Validation, Resources, Writing – review & editing, Supervision, Funding acquisition.

Declaration of competing interest

The authors declare that they have no known competing financial interests or personal relationships that could have appeared to influence the work reported in this paper.

Acknowledgments

The authors would like to thank Fundação para a Ciência e a Tecnologia (FCT) for funding the present research via project grants PTDC/CTA-AMB/30056/2017 (OPTOX), UIDB/04292/2020 (MARE), UIDB/04326/2020 (CCMAR), as well as UIDP/04046/2020 (BioISI). B. Duarte was supported by an FCT investigator contract (CEECIND/00511/2017), and J. Roma was supported by a PhD grant (SFRH/BD/138318/2018). Lastly the authors thank the project PORTWIMS (Portugal Twinning for Innovation and Excellence in Marine Science and Earth Observation), which was co-funded by the European Union's Horizon 2020 research and innovation programme under grant agreement No 810139. We would also like to thank to Dr. Johannes Goessling for his assistance in nanoparticle characterization.

References

Alkanani, T., Parrish, C.C., Thompson, R.J., McKenzie, C.H., 2007. Role of fatty acids in cultured mussels, Mytilus edulis, grown in notre Dame Bay, Newfoundland. J. Exp. Mar. Biol. Ecol. 348, 33–45.

Avila, I.C., Kaschner, K., Dormann, C.F., 2018. Current global risks to marine mammals: taking stock of the threats. Biol. Conserv. 221, 44–58.

Baker, T.J., Tyler, C.R., Galloway, T.S., 2014. Impacts of metal and metal oxide nanoparticles on marine organisms. Environ. Pollut. 186, 257–271.

Barnathan, G., 2009. Non-methylene-interrupted fatty acids from marine invertebrates: occurrence, characterization, and biological properties. Biochimie 91 (6), 671–678.

Berge, J., Barnathan, G., 2005. Fatty acids from lipids of marine organisms: molecular biodiversity, roles as biomarkers, biologically active compounds, and economical aspects. Mar. Biotechnol. I 96, 49–125.

Bhatt, I., Tripathi, B.N., 2011. Interaction of engineered nanoparticles with various components of the environment and possible strategies for their risk assessment. Chemosphere 82, 308–317.

Boening, D.W., 1999. An evaluation of bivalves as biomonitors of heavy metals pollution in marine waters. Environ. Monit. Assess. 55, 459–470.

Brayner, R., Ferrari-Iliou, R., Brivois, N., Djediat, S., Benedetti, M.F., Fievet, F., 2006. Toxicological impact studies based on Escherichia coli bacteria in ultrafine ZnO nanoparticles colloidal medium. Nano Lett. 6, 866–870.

Brouwer, I.A., Geelen, A., Katan, M.B., 2006. N-3 fatty acids, cardiac arrhythmia and fatal coronary heart disease. Prog. Lipid Res. 45, 357–367.

Calder, P.C., 2015. Functional roles of fatty acids and their effects on human health. J. Parenter. Enter. Nutr. 39, 18S–32S.

Calder, P.C., 2018. Very long-chain n -3 fatty acids and human health: fact, fiction and the future. Proc. Nutr. Soc. 77, 52–72.

Chong, K., Wang, W.X., 2009. Assimilation of cadmium, chromium, and zinc by the green mussel Perna viridis and the clam ruditapes philippinarum. Environ. Toxicol. Chem. 19 (6), 1660–1667.

Clarke, Gorley, 2006. PRIMER v6: user manual/tutorial. PRIMER-E.

Coll, C., Notter, D., Gottschalk, F., Sun, T., Som, C., Nowack, B., 2016. Probabilistic environmental risk assessment of five nanomaterials (nano-TiO2, nano-Ag, nano-ZnO, CNT, and fullerenes). Nanotoxicology 10, 4.

Cruz de Carvalho, R., Feijão, E., Matos, A.R., Cabrita, M.T., Novais, S.C., Lemos, M.F., Caçador, I., Marques, J.C., Reis-Santos, P., Fonseca, V.F., Duarte, B., 2020. Glyphosate-based herbicide toxicophenomics in marine diatoms: impacts on primary production and physiological fitness. Appl. Sci. 10 (21), 7391.

Dailianis, S., 2011. Environmental impact of anthropogenic activities: the use of mussels as a reliable tool for monitoring marine pollution. In: McGevin, L.E. (Ed.), Mussels: Anatomy. Habitat and Environmental Impact. Nova Science Publishers, Inc, pp. 1–30.

DeCaterina, Basta, 2001. n-3 Fatty acids and the inflammatory response – biological background. Eur. Heart J. Suppl. 3 (D), 42–49.

Dernekbaşı, S., Öksüz, A., Çelik, M.Y., Karayücel, İ., Karayücel, S., 2015. The fatty acid composition of cultured mussels (Mytilus galloprovincialis lamarck 1819) in offshore longline system in the Black Sea. J. Aquac. Mar. Biol. 2 (6), 46–53.

Duarte, B., Prata, D., Matos, A., Rita, Cabrita, M., Teresa, 2019. Ecotoxicity of the lipid-lowering drug bezafibrate on the bioenergetics and lipid metabolism of the diatom Phaeodactylum tricornutum. Sci. Total Environ. 650, 2085–2094.

Duarte, B., Feijão, E., Cruz de Carvalho, R., Duarte, I.A., Silva, M., Matos, A.R., Cabrita, M.T., Novais, S.C., Lemos, M.F., Marques, J.C., Caçador, I., 2020. Effects of propranolol on growth, lipids and energy metabolism and oxidative stress response of Phaeodactylum tricornutum. Biology 9 (12), 478.

Duarte, B., Carreiras, J., Feijão, E., Reis-Santos, P., Caçador, I., Matos, A.R., Fonseca, V.F., 2021a. Fatty acid profiles of estuarine macroalgae are biomarkers of anthropogenic pressures: development and application of a multivariate pressure index. Sci. Total Environ. 788, 147817.

Duarte, B., Feijão, E., Goessling, J.W., Caçador, I., Matos, A.R., 2021b. Pigment and fatty acid production under different light qualities in the diatom Phaeodactylum tricornutum. Appl. Sci. 11 (6), 2550.

Duroudier, et al., 2019. Changes in protein expression in mussels Mytilus galloprovincialis dietarily exposed to PVP/PEI coated silver nanoparticles at different seasons. Aquat. Toxicol. 210, 56–68.

Fabrega, J., Tantra, R., Amer, A., Stolpe, B., Tomkins, J., Fry, T., Lead, J.R., Tyler, C.R., Galloway, T.S., 2012. Sequestration of zinc from zinc oxide nanoparticles and life cycle effects in the sediment dweller amphipod Corophium volutator. Environ. Sci. Technol. 46 (2), 1128–1135.

Falk-Petersen, S., Hagen, W., Kattner, G., Clarke, A., Sargent, J., 2000. Lipids, trophic relationships, and biodiversity in Arctic and Antarctic krill. Can. J. Fish. Aquat. Sci. 57, 178–191.

Feijão, E., Gameiro, C., Franzitta, M., Duarte, B., Caçador, I., Cabrita, M., et al., 2018. Heat wave impacts on the model diatom Phaeodactylum tricornutum: searching for photochemical and fatty acid biomarkers of thermal stress. Ecol. Indicat. 95, 1026–1037.

Feijão, E., Franzitta, M., Cabrita, M.T., Caçador, I., Duarte, B., Gameiro, C., Matos, A.R., 2020. Marine heat waves alter gene expression of key enzymes of membrane and storage lipids metabolism in Phaeodactylum tricornutum. Plant Physiol. Biochem. 156, 357–368.

Fokina, N.N., Ruokolainen, T.R., Nemova, N.N., Bakhmet, I.N., 2013. Changes of blue mussels Mytilus edulis L. Lipid composition under cadmium and copper toxic effect. Biol. Trace Elem. Res. 154 (2), 217–225.

Fonseca, V.F., Duarte, I.A., Matos, A.R., Reis-Santos, P., Duarte, B., 2021. Fatty acid profiles as natural tracers of provenance and lipid quality indicators in illegally sourced fish and bivalves. Food Control 134, 108735.

Fox, C.H., O'Hara, P.D., Bertazzon, S., Morgan, K., Underwood, F.E., Paquet, P.C., 2016. A preliminary spatial assessment of risk: marine birds and chronic oil pollution on Canada's Pacific coast. Sci. Total Environ. 573, 799–809.

Franzitta, M., Feijão, E., Cabrita, M.T., Gameiro, C., Matos, A.R., Marques, J.C., Goessling, J.W., Reis-Santos, P., Fonseca, V.F., Pretti, C., Caçador, I., Duarte, B., 2020. Toxicity going nano: ionic versus engineered cu nanoparticles (ENPs) impacts on the physiological fitness of the model diatom Phaeodactylum tricornutum. Front. Mar. Sci. 7, 539827.

Freites, L., Fernández-Reiriz, M.J., Labarta, U., 2002. Fatty acid profiles of Mytilus galloprovincialis (Lmk) mussel of subtidal and rocky shore origin. Comp. Biochem. Physiol. B: Biochem. Mol. Biol. 132 (2), 453–461.

Garaffo, M.A., Vassallo-Agius, R., Nengas, Y., Lembo, E., Rando, R., Maisano, R., Dugo, G., Giuffrida, D., 2011. Fatty acids profile, atherogenic (IA) and thrombogenic (IT) health lipid indices, of raw roe of blue fin tuna (Thunnus thynnus L.) and their salted product "Bottarga". Food Nutr. Sci. 2, 736–743.

Gennis, R.B., 1989. Biomembranes: Molecular Structure and Function. Springer ISBN 0387967605.

Goldberg, E.D., 1986. The mussel watch concept. Environ. Monit. Assess. 7, 91–103.

Gottschalk, F., et al., 2009. Modeled environmental concentrations of engineered nanomaterials (TiO2, ZnO, Ag, CNT, fullerenes) for different regions. Environ. Sci. Technol. 43 (9216–9222).

Graeve, M., Hagen, W., Kattner, G., 1994. Herbivorous or omnivorous? On the significance of lipid compositions as trophic markers in Antarctic copepods. Deep Sea Res. 41, 915–924.

Graeve, M., Kattner, G., Piepenburg, D., 1997. Lipids in Arctic benthos: does the fatty acid and alcohol composition reflect feeding and trophic interactions? Polar Biol. 18, 53–61.

Hanna, S., et al., 2013. Impact of engineered zinc oxide nanoparticles on the individual performance of Mytilus galloprovincialis. PLoS One 8 (4), e61800.

Hannam, M.L., Bamber, S.D., Galloway, T.S., John Moody, A., Jones, M.B., 2010. Effects of the model PAH phenanthrene on immune function and oxidative stress in the haemolymph of the temperate scallop Pecten maximus. Chemosphere 78, 779–784.

Hodges, D., DeLong, J., Forney, C., Prange, R., 1999. Improving the thiobarbituric acid-reactive-substances assay for estimating lipid peroxidation in plant tissues containing anthocyanin and other interfering compounds. Planta 207 (4), 604–611.

Iversen, T.G., Skotland, T., Sandvig, K., 2011. Endocytosis and intracellular transport of nanoparticles: present knowledge and need for future studies. Nano Today 6 (2), 176–185.
Kaneda, T., 1967. Fatty acids in the genus bacillus. I. Iso and anteiso-fatty acids as characteristic constituents of lipids in 10 species. J. Bacteriol. 93, 894–903.
Keller, A.A., et al., 2013. Global life cycle releases of engineered nanomaterials. J. Nanopart. Res. 15 (1692).
Kharlamenko, V.I., Kiyashko, S.I., Imbs, A.B., Vyshkvartzev, D.I., 2001. Identification of food source of invertebrates from the seagrass Zostera marina community using carbon and Sulphur stable isotope ratio and fatty acid analyses. Mar. Ecol.-Prog. Ser. 220, 103–117.
Klingensmith, J.S., 1982. Distribution of methylene and non methylene-interrupted dienoic fatty acids in polar lipids and triacylglycerols of selected tissue of the hard-shell clam (Mercenaria mercenaria). Lipids 17, 976–981.
Kraffe, F., Soudant, P., Marty, Y., 2004. Fatty acids of serine, ethanolamine, and choline plasmalogens in some marine bivalves. Lipids 39, 59–66.
Labarta, U., Fernandez-Reiriz, M.J., Perez-Camacho, A., 1999. Dynamic of fatty acids in the larval development, metamorphosis and post-metamorphosis of Ostrea edulis (L.). Comp. Biochem. Physiol. A 123, 249–254.
Labarta, U., Fernández-Reiriz, M.J., Garrido, J.L., Babarro, M.F., Bayona, J.M., Albaigés, J., 2005. Response of mussel recruits to pollution from the 'Prestige' oil spill along the Galicia coast. A biochemical approach. Mar. Ecol. Prog. Ser. 302, 135–145.
Lachance, A.A., Myrand, B., Tremblay, R., Koutitonsky, V., Carrington, E., 2008. Biotic and abiotic factors influencing attachment strength of blue mussels Mytilus edulis in suspended culture. Aquat. Biol. 2, 119–129.
Langdon, C.J., Waldock, M.J., 1981. The effect of algal and artificial diets on the growth and fatty acid composition of Crassostrea gigas spat. J. Mar. Biol. Assoc. UK 61, 441–448.
Li, J., Schiavo, S., Xiangli, D., Rametta, G., Miglietta, M.L., Oliviero, M., Changwen, W., Manzo, S., 2018. Early ecotoxic effects of ZnO nanoparticle chronic exposure in Mytilus galloprovincialis revealed by transcription of apoptosis and antioxidant-related genes. Ecotoxicology 27 (3), 369–384.
Lin, D.H., Xing, B.S., 2007. Phytotoxicity of nanoparticles: inhibition of seed germination and root growth. Environ. Pollut. 150, 243–250.
Mansom, B., Grover, E., 2018. Mussels: Characteristics, Biology and Conservation. Nova Science Publishers, New York.
Manzo, S., Miglietta, M.L., Rametta, G., Buono, S., Di Francia, G., 2013. Toxic effects of ZnO nanoparticles towards marine algae Dunaliella tertiolecta. Sci. Total Environ. 445, 371–376.
Markert, B.A., Breure, A.M., Zechmeister, H.G., 2003. Bioindicators and Biomonitors. first ed. Elsevier, Oxford.
Monroig, Ó., Kabeya, N., 2018. Desaturases and elongases involved in polyunsaturated fatty acid biosynthesis in aquatic invertebrates: a comprehensive review. Fish. Sci. 84 (6), 911–928.
Murphy, K.J., Money, B.D., Mann, N.J., Nichols, P.D., Sinclair, A.J., 2002. Lipid FA, and sterol composition of New Zealand gren lipped mussel (Perna canaliculus) and tasmanian blue mussel (Mytilus edulis). Lipids 37 (6), 587–595.
Nadella, S.R., Fitzpatrick, J.L., Franklin, N., Bucking, C., Smith, S., Wood, C.M., 2009. Toxicity of dissolved cu, zn, ni and cd to developing embryos of the blue mussel (Mytilus trossolus) and the protective effect of dissolved organic carbon. Comp. Biochem. Physiol., Part C: Toxicol. Pharmacol. 149 (3), 340–348.
Nielsen, T.G., Maar, M., 2007. Effects of a blue mussel Mytilus edulis bed on vertical distribution and composition of the pelagic food web MEPS. 339, 185–198.
OECD, 2009. Nanotechnology: an overview based on indicators and statistics. https://www.oecd-ilibrary.org/science-and-technology/nanotechnology-an-overview-based-on-indicators-and-statistics_223147043844?crawler=true accessed 20 May 2021.
Ofiara, D.D., Seneca, J.J., 2006. Biological effects and subsequent economic effects and losses from marine pollution and degradations in marine environments: implications from the literature. Mar. Pollut. Bull. 52, 844–864.
Osmond, M.J., McCall, M.J., 2010. Zinc oxide nanoparticles in modern sunscreens: an analysis of potential exposure and hazard. Nanotoxicology 4, 15–41.
Parkes, R.J., Taylor, J., 1983. The relationship between fatty acid distributions and bacterial respiratory types in contemporary marine sediments. Estuar. Coast. Shelf Sci. 16, 173–189.
Parks, A.N., Portis, L.M., Schierz, P.A., Washburn, K.M., Perron, M.M., Burgess, R.M., Ho, K.T., Chandler, G.T., Ferguson, P.L., 2013. Bioaccumulation and toxicity of single-walled carbon nanotubes to benthic organisms at the base of the marine food chain. Environ. Toxicol. Chem. 32 (6), 1270–1277.
Parrish, C.C., 2009. Essential fatty acids in aquatic food webs. Lipids in Aquatic Ecosystems, pp. 309–326.
Pazos, J.A., Roman, G., Acosta, C.P., Sanchez, J.L., Abad, M., 1997. Lipid classes and fatty acid composition in the female gonad of Pecten maximus in relation to reproductive cycle and environmental variables. Comp. Biochem. Physiol. B 117, 393–402.
Perry, G., Volkman, J.K., Johns, R.B., 1979. Fatty acid of bacterial origin in contemporary marine sediments. Geochim. Cosmochim. Acta 43, 1715–1725.
Prato, E., Danieli, A., Maffia, M., Biandolino, F., 2010. Lipid and fatty acid compositions of Mytilus galloprovincialis cultured in the mar grande of Taranto (Southern Italy): feeding strategies and trophic relationships. Zool. Stud. 49 (2), 211–219.
Premanathan, M., Karthikeyan, K., Jeyasubramanian, K., Manivannan, G., 2011. Se- lective toxicity of ZnO nanoparticles toward gram-positive bacteria and cancer cells by apoptosis through lipid peroxidation. Nanomed. Nanotechnol. Biol. Med. 7, 184–192.
Pryor, A.W., Stanley, P., 1975. A suggested mechanism for the production of malonaldehyde during the autooxidation of poly-unsaturated fatty acids. Nonenzymatic production of prostaglandin endoperoxides during autooxidation. J. Org. Chem. 40, 3615–3617.
Rainbow, P.S., Phillips, D.J.H., 1993. Cosmopolitan biomonitors oftrace metals. Mar. Pollut. Bull. 11, 593–601.
Rainbow, P.S., Smith, B.D., Lau, S.S.S., 2002. Biomonitoring of trace metal availabilities in the Thames estuary using a suite of littoral biomonitors. J. Mar. Biol. Assoc. U. K. 82 (5), 793–799.
Reddy, K.M., Feris, K., Bell, J., Wingett, D.G., Hanley, C., Punnoose, A., 2007. Selective toxicity of zinc oxide nanoparticles to prokaryotic and eukaryotic systems. Appl. Phys. Lett. 90, 2139021–2139023.
Rocchetta, I., Pasquevich, M.Y., Heras, H., Ríos de Molina, M.D.C., Luquet, C.M., 2014. Effects of sewage discharges on lipid and fatty acid composition of the Patagonian bivalve Diplodon chilensis. Mar. Pollut. Bull. 79, 211–219.
Roma, J., Matos, A.R., Vinagre, C., Duarte, B., 2020. Engineered metal nanoparticles in the marine environment: a review of the effects on marine fauna. Mar. Environ. Res. 161, 105110.
Santos, D., Duarte, B., Caçador, I., 2014. Unveiling zn hyperacumulation in Juncus acutus: implications on the electronic energy fluxes and on oxidative stress with emphasis on non-functional zn-chlorophylls. J. Photochem. Photobiol. B Biol. 140, 228–239.
Schrand, Amanda M., Rahman, Mohammad F., Hussain, Saber M., Schlager, John J., Smith, David A., Syed, Ali F., 2010.. Metal-based nanoparticles and their toxicity assessment. Wiley Interdiscip. Rev. Nanomed. Nanobiotechnol. 2 (5), 544–568 (09-01).
Sghaier, D.B., Pedro, S., Diniz, M.S., Duarte, B., Caçador, I., Sleimi, N., 2016. Tissue localization and distribution of as and Al in the halophyte Tamarix gallica under controlled conditions. Front. Mar. Sci. 3, 274.
Signa, G., Di Leonardo, R., Vaccaro, A., Tramati, C.D., Mazzola, A., Vizzini, S., 2015. Lipid and fatty acid biomarkers as proxies for environmental contamination in caged mussels Mytilus galloprovincialis. Ecol. Indic. 57, 384–394.
Sunda, W.G., Engel, D.W., Thuotte, R.M., 1978. Effect of chemical speciation on toxicity of cadmium to grass shrimp, Palaemonetes pugio: importance of free cadmium ion. Environ. Sci. Technol. 12 (4), 409–413.
Taze, C., Panetas, I., Kalogiannis, S., Feidantsis, K., Gallios, G.P., Kastrinaki, G., Konstandopoulos, A.G., Václavíková, M., Ivanicova, L., Kaloyianni, M., 2016. Toxicity assessment and comparison between two types of iron oxide nanoparticles in Mytilus galloprovincialis. Aquat. Toxicol. 172, 9–20.
Towett, E.K., Shepherd, K.D., Cadisch, G., 2013. Quantification of total element concentrations in soils using total X-ray fluorescence spectroscopy (TXRF). Sci. Total Environ. 463–464, 374–388.
Ulbricht, T.L., Southgate, D.A.T., 1991. Coronary heart disease: seven dietary factors. Lancet 338, 985–992.
Valko, M., Morris, H., Cronin, M.T.D., 2005. Metals, toxicity, and oxidative stress. Curr. Med. Chem. 12, 1161–1208.
Van Sprang, P.A., Verdonck, F.A.M., Van Assche, F., Regoli, L., De Schamphelaere, K.A.C., 2009. Environmental risk assessment of zinc in european freshwaters: a critical appraisal. Sci. Total Environ. 407 (20), 5373–5391.
Ventrella, V., Pirini, M., Pagliarani, A., Trombetti, F., Manuzzi, M.P., et al., 2008. Effect of temporal and geographical factors on fatty acid composition of M. Galloprovincialis from the Adriatic Sea. Comp Biochem Physiol B Biochem Mol Biol 149 (2), 241–250.
Viarengo, A., Lowe, D., Bolognesi, C., Fabbri, E., Koehler, A., 2007. The use of biomarkers in biomonitoring: a 2-tier approach assessing the level of pollutant-induced stress syndrome in sentinel organisms. Comp. Biochem. Physiol. C: Toxicol. Pharmacol. 146, 281–300. https://doi.org/10.1016/j.cbpc.2007.04.011.
Vignardi, C.P., Hasue, F.M., Sartório, P.V., Cardoso, C.M., Machado, A.S., Passos, M.J., Gomes, V., 2015. Genotoxicity, potential cytotoxicity and cell uptake of titanium dioxide nanoparticles in the marine fish Trachinotus carolinus (Linnaeus, 1766). Aquat. Toxicol. 158, 218–229.
Vlahogianni, T.H., Valavandis, A., 2007. Heavy-metal effects on lipid peroxidation and antioxidant defense enzymes in mussels Mytilus galloprovincialis. Chem. Ecol. 5, 361–371.
Wang, B., Feng, W.Y., Wang, M., Wang, T.C., G.U., Y.Q., Zhu, M.T., Ouyang, H., Shi, J.W., Zhang, F., Zhao, Y.L., Chai, Z.F., Wang, H.F., Wang, J., 2008. Acute toxicological impact of nano- and submicro-scaled zinc oxide powder on healthy adult mice. J. Nanopart. Res. 10, 263–276.
Wong, S.W., Leung, K.M., 2014. Temperature-dependent toxicities of nano-zinc oxide to marine diatom, amphipod and fish in relation to its aggregation size and ion dissolution. Nanotoxicology 8 (sup1), 24–35.
Wong, S.W., Leung, P.T., Djurišic, A.B., Leung, K.M., 2010. Toxicities of nano-zinc oxide to five marine organisms: influences of aggregate size and ion solubility. Anal. Bioanal. Chem. 396 (2), 609–618.
Zamuda, C.D., Sunda, W.G., 1982. Bioavailability of dissolved copper to the American oyster Crassostrea virginica. I. Importance of chemical speciation. Mar. Biol. 66 (1), 77–82.
Zhukova, N.V., 1991. The pathway of the biosynthesis of nonmethylene-interrupted dienoic fatty acids in mollusks. Comp. Biochem. Physiol. B 100 (4), 801–804.